

# Droplet nucleation and Smoluchowski's equation with growth and injection of particles

Stéphane Cueille and Clément Sire

Laboratoire de Physique Quantique, UMR C5626 du CNRS, Université Paul Sabatier, 31062 Toulouse Cedex, France

(Received 27 June 1997; revised manuscript received 23 September 1997)

We show that models for homogeneous and heterogeneous nucleation of  $D$ -dimensional droplets in a  $d$ -dimensional medium are described in the mean field by a modified Smoluchowski equation for the distribution  $N(s,t)$  of droplet masses  $s$ , with additional terms accounting for exogenous growth from vapor absorption and injection of small droplets when the model allows renucleation. The corresponding collision kernel is derived in both cases. For a generic collision kernel  $K$ , the equation describes a clustering process with clusters of mass  $s$  growing between collision with  $\dot{s} \propto s^\beta$  and injection of monomers at a rate  $I$ . General properties of this equation are studied. The gel criterion is determined. Without injection, exact solutions are found with a constant kernel, exhibiting unusual scaling behavior. For a general kernel, under the scaling assumption  $N(s,t) \sim Y(t)^{-1} f(s/S(t))$ , we determine the asymptotics of  $S(t)$  and  $Y(t)$  and derive the scaling equation. Depending on  $\beta$  and  $K$ , a great diversity of behaviors is found. For constant injection, there is an asymptotic steady state with  $N(s,t \rightarrow \infty) \propto s^{-\tau}$  and  $\tau$  is determined. The case of a constant mass injection rate is related to homogeneous nucleation and studied. Finally, we show how these results shed some light on heterogeneous nucleation with  $d=D$ . For  $d=D=2$  (disks on a plane), numerical simulations are performed, in good agreement with the mean-field results. [S1063-651X(98)09401-X]

PACS number(s): 64.60.Qb, 02.50.-r, 82.20.Mj

## I. INTRODUCTION

Aggregation models are relevant to describe a great diversity of practically important physical phenomena in fields ranging from atmosphere sciences to cosmology, including material sciences and chemical engineering [1–4]. A remarkable example is *dropwise condensation* on a substrate [5], for instance, water on a cold window pane, which bears on important implications in heat transfer engineering and material sciences and generates fascinating droplet patterns, also called *breath figures* [6]. Although the underlying physics is rich (see [5]), simplified aggregation models have been successfully introduced to simulate the late stage of droplet growth and coalescence [5,7–13]. These models are of basically two kinds. On the one hand, in *heterogeneous nucleation* models, one starts from a fixed number of nucleation sites (in physical situations these might be dust particles, substrate defects, etc.). Droplets grow on these sites through vapor absorption, and when two neighboring droplets overlap, they coalesce to form a single droplet, thus reducing the number of droplets. On the other hand, in *homogeneous growth* models [8], nucleation can occur anywhere on the substrate: Some very small droplets are randomly deposited, which leads to the growth of existing droplets and the creation of new small droplets if deposition occurs in a free zone.

Experiments and numerical simulations [5,9] show that the time-dependent droplet mass distribution  $N(s,t)$  ( $s$  being the mass of the droplets), exhibits dynamic scaling, i.e., that for long times  $N(s,t) \propto S(t)^{-\theta} f(s/S(t))$ .  $S(t)$  is a typical droplet mass (proportional to  $\langle s^2 \rangle / \langle s \rangle^2$ ) and has a power-law divergence at long times  $S(t) \propto t^z$ .  $\theta$  and  $z$  are dynamic exponents that depend not on the fine details of the model but only on its main features, such as its conservation laws. In heterogeneous growth models, the scaling function  $f(x)$  is narrow, whereas in homogeneous growth one observes the

superposition of a narrow distribution of large droplets [with masses of the same order as  $S(t)$ ], and a broad distribution of small droplets with a power-law divergence of the scaling function  $f(x) \propto x^{-\tau}$  at small  $x$ .  $\tau$  is nontrivial and less than  $\theta$  [9].

A complete theoretical understanding of these results is still lacking and the prediction of the *polydispersity exponent*  $\tau$  is a challenge. Most analytical treatments concern heterogeneous growth and start from the assumption that the distribution of masses is narrow [7,12]. Therefore, a theory for the distribution function, describing at least simplified computer models, is highly desirable to get free of this assumption in the case of heterogeneous growth and to be able to treat homogeneous nucleation.

As far as standard aggregation models, such as diffusion-limited cluster aggregation [14,15], are concerned, a great deal of information can be gained from Smoluchowski's mean-field approach [16]: Neglecting fluctuations and multiple collisions, one can write down a rate equation

$$\partial_t N(s,t) = \frac{1}{2} \int N(s_1,t) N(s-s_1,t) K(s_1, s-s_1) ds_1 - N(s,t) \int N(s_1,t) K(s, s_1) ds_1, \quad (1.1)$$

where the collision kernel  $K(s_1, s_2)$  is the coalescence rate between droplets of masses  $s_1$  and  $s_2$ . Smoluchowski's approach is valid above an upper critical dimension, which is often 2, but is in principle model dependent [17]. van Dongen and Ernst [18], classified the kernels according to their homogeneity and asymptotic behavior:

$$K(bx, by) = b^\lambda K(x, y), \quad (1.2)$$

$$K(x, y) \sim x^\mu y^{\lambda - \mu} (y \gg x). \quad (1.3)$$

Nontrivial polydispersity exponents appear in the case  $\mu=0$  [18–20], whereas for  $\mu>0$ ,  $\tau$  is equal to  $1+\lambda$  and for  $\mu<0$  the distribution is bell shaped.

However, Eq. (1.2) does not describe aggregation models, such as droplets nucleation models, for which clusters not only grow through collisions (coalescence) but also collect some mass from the “outside” (vapor) between collisions. Hence an adaptation of Smoluchowski’s approach to treat breath figures and related models is required and is the purpose of the present work. The article is organized as follows.

In Sec. II we discuss nucleation models introduced by Family and Meakin [9] and derive the corresponding Smoluchowski equation under the mean-field assumption. In the generalized Smoluchowski equation, an additional exogenous growth term  $\partial_s(s^\beta N)$  on the left-hand side of Eq. (1.1) accounts for clusters growing between collisions with  $\dot{s} \propto s^\beta$  (*exogenous growth*), while a time-dependent source term  $I(t)\delta(s-s_0)$  describes renucleation in empty spaces.

Section III is a *general* study of the extended Smoluchowski equation corresponding to aggregation with *cluster exogenous growth* and *injection* with a *generic* homogeneous *kernel*. First, we investigate the gelation criterion, depending on  $\lambda$  defined in Eq. (1.2), and show that the system is non-gelling for  $\max(\lambda, \beta) \leq 1$ . Then we focus on the case without injection ( $I=0$ ). We exhibit some exact solutions ( $K=1$ , with  $\beta=0$  or  $\beta=1$ ). We study extensively the properties of the scaling solutions, depending on  $\beta$ ,  $\lambda$ , and  $\mu$ . The competition between collisions and exogenous growth leads to a much richer behavior than for standard Smoluchowski’s equation. We pay special attention to the occurrence of polydispersity exponents and show that the methods recently introduced by the present authors [20] can be directly used to compute nontrivial  $\tau$  exponents when they appear.

Returning to  $I>0$ , we first consider constant injection of monomer. We find that the distribution reaches at an infinite time a polydisperse steady state with a power-law large- $s$  decay  $N_\infty(s) \propto s^{-\tau}$ , with  $\tau=(3+\lambda)/2$  if  $\beta<(1+\lambda)/2$  and  $\tau=2+\lambda-\beta$  if  $\beta>(1+\lambda)/2$ . Then we consider the more specific case, relevant to homogeneous nucleation, of a constant mass injection rate [with a self-consistent  $I(t)$ ] and  $\lambda=2\beta-1$ . We show that the injection rate  $I(t)$  is vanishing, in agreement with the droplet model. We also investigate scaling solutions and suggest that including pair correlations may be necessary to find a consistent scaling for homogeneous growth.

In Sec. IV we apply the scaling mean-field results to heterogeneous growth with  $d=D$ . Droplets radii  $r=s^{1/D}$  grow as  $\dot{r} \propto r^\omega$  [ $\beta=1+(\omega-1)/D$ ] and a nontrivial polydispersity exponent  $\tau$  occurs for  $\omega \geq 0$ , while the scaling function vanishes at a small argument for  $\omega<0$ . Mean-field polydispersity exponents are computed using the variational method introduced in [20]. Numerical results for the scaling function are in qualitative agreement with mean-field results and the expected crossover from monodispersity to polydispersity at  $\omega=0$  is observed.

Note that throughout the article, we shall use the words “polydisperse” and “monodisperse” in a quite specific sense. A mass distribution will be *polydisperse* if the scaling

function  $f(x)$  diverges when  $x \rightarrow 0$ . If  $f(x) \rightarrow 0$  (bell-shaped distribution), it will be *monodisperse*. When all clusters have exactly the same mass, we shall say that their mass distribution is *strictly* monodisperse.

Part of the results concerning the case without injection have already appeared in a summarized form in [21].

## II. DROPLET DEPOSITION, GROWTH, AND COALESCENCE IN THE MEAN FIELD

As mentioned in the Introduction, interest in droplet nucleation computer models was primarily aroused by practical applications in heat transfer engineering (see references in [5]). In the past ten years, however, and since the seminal work of Beysens and Knobler [6], the focus was set on the formation of breath figures (see figures in [5]), with computer models aimed to study the kinetics of the droplet mass distribution [8–10,12,5], the asymptotic surface (or line) coverage [11], or the time evolution of the “dry” fraction (the surface fraction that has never been covered by any droplet) [13].

In this article we shall consider the specific models introduced by Family and Meakin [8,9] for both homogeneous and heterogeneous nucleation. We shall now describe these models and derive the corresponding Smoluchowski equation. These equations are special cases of a generalized Smoluchowski equation, which will be studied in Sec. III.

### A. Homogeneous nucleation

The *deposition and coalescence* model [8] consists in the following algorithm. Between  $t$  and  $t+\delta t$  a small droplet of mass  $s_0$  is randomly deposited on the  $d$ -dimensional substrate, where it forms a spherical cap with radius  $s_0^{1/D}$ . If it overlaps an existing droplet of mass  $s$ , they coalesce to form a new droplet with mass  $s+s_0$  and radius  $(s+s_0)^{1/D}$ , centered at the center of mass of the two coalescing droplets. If the new droplet overlaps a surrounding droplet, they coalesce with the same rule, and so on.

Snapshots of droplets configurations obtained by simulation of the deposition and coalescence model for  $d=2$  and  $D=3$  are qualitatively very close to the one obtained in some experiments of vapor deposition of thin films [9]. The striking feature is the coexistence of two distinct populations of droplets: a population of big droplets, with essentially the same mass, surrounded by a population of smaller droplets with a broad dispersion of masses. At late times, the distribution of droplet masses  $N(s, t)$  exhibits dynamic scaling,

$$N(s, t) \sim S(t)^{-\theta} f(s/S(t)), \quad (2.1)$$

where the typical mass scale  $S(t)$  can be defined by

$$S(t) = \frac{\langle s^2 \rangle}{\langle s \rangle} = \frac{\int s^2 N(s, t)}{\int s N(s, t)}. \quad (2.2)$$

The dynamical exponents  $\theta$  and  $z$  can be determined from physical arguments [5,9]. Since the mass injection rate is constant and the mass is conserved in the coalescence process, we must have

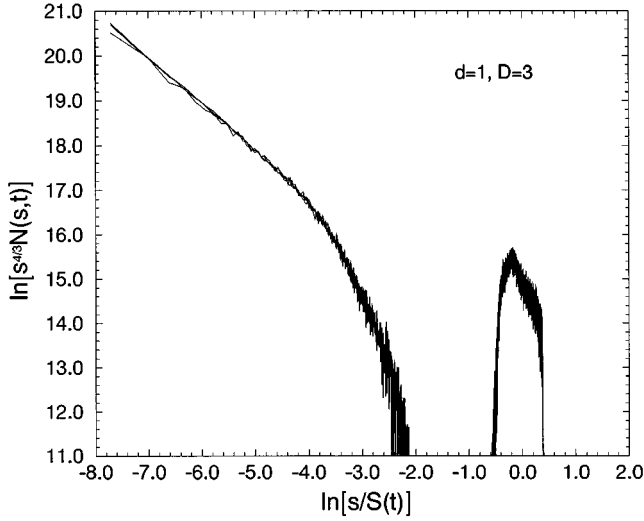


FIG. 1. Scaling of the mass distribution  $N(s,t)$  for droplet deposition with  $d=1$  and  $D=3$ . The picture shows the excellent data collapse, with the theoretical value  $4/3$  for  $\theta$ , of the distribution at four different times when  $S$  has reached the values 6053, 11 116, 15 539, and 17 112, respectively. The scaling function is composed of a polydisperse contribution of small droplets and a monodisperse contribution of droplets of mass of order  $S(t)$ .

$$t \int_0^{+\infty} s N(s,t) ds \propto S(t)^{2-\theta} \int_0^{+\infty} x f(x) dx, \quad (2.3)$$

which, from the definition of  $z$ , implies the scaling law  $z(2 - \theta) = 1$ . Then we note that the fraction of substrate “area” occupied by the droplets is

$$\int_0^{+\infty} s^{d/D} N(s,t) ds \propto S(t)^{1+d/D-\theta} \quad (2.4)$$

and cannot diverge or vanish, so that  $\theta = 1 + d/D$ . From the scaling law, we get  $z = D/(D-d)$ .

The scaling behavior of the total number of droplets  $n(t)$  depends on the small- $x$  behavior of the scaling function  $f(x)$ .

If the scaling function is integrable in zero, it is easily seen that  $n(t) \propto S(t)^{1-\theta}$ , whereas if  $f(x) \propto x^{-\tau}$  with  $\tau > 1$ ,  $n(t) \propto S(t)^{\tau-\theta}$ .

In [9] excellent scaling was obtained with the theoretical value of  $\theta$  for various  $d$  and  $D$ . Measured values of  $z$  are also fully consistent with the theory. As an illustration, a typical scaling function is shown in Fig. 1 from our simulations in  $d=1$  with  $D=3$ . The data collapse is obtained with the theoretical value  $\theta=4/3$ . The scaling function is clearly bimodal. A broad droplet distribution, with a small-argument divergence of the scaling function associated with an exponent  $\tau$  bigger than 1, is well separated from a bell-shaped distribution of bigger droplets centered around  $s=S(t)$ . Following the definitions given in the Introduction, we shall say that the scaling function of the population of small (big) droplets is *polydisperse* (*monodisperse*). Most of the droplets in the system contribute to the small droplets distribution, which determines, since  $\tau > 1$ , the behavior of  $n(t)$ , whereas the population of bigger droplets contains most of the mass and  $S(t)$  is the typical mass of big droplets.

In [9] the polydispersity exponent  $\tau$  was determined directly from the numerical determination of the scaling function, but with important uncertainty due to statistical limitations, and it may be better to extract  $\tau$  from  $n(t) \propto [S(t)]^{(\tau-\theta)}$ . In all cases it is found that  $1 < \tau < \theta$  [for instance, our simulations in  $d=1$  yield  $\tau=1.264 < 3/2$  ( $D=2$ ),  $\tau=1.18 < 4/3$  ( $D=3$ ), and  $\tau=1.074 < 5/4$  ( $D=4$ )]. The value of  $\tau$  does not seem to be simply related to  $d$  and  $D$ . Such nontrivial polydispersity exponents are quite frequent in aggregation models and occur even in the mean field through Smoluchowski's equation, as mentioned in the Introduction. Therefore, it is interesting to derive a Smoluchowski equation for this model and check the mean-field value of  $\tau$ , if possible.

Family and Meakin [9] showed from scaling arguments that the coalescence kernel should have a homogeneity  $\lambda = 2d/D - 1$ , but they did not determine its specific form. We proceed now to the derivation of the equation. Neglecting multiple collisions, we examine the different events affecting the distribution  $N(s,t)$ .

Between  $t$  and  $t+1$ , a droplet of radius  $s = ks_0$  is created as the outcome of the following processes.

(i) A droplet of mass  $s_0$  falls on a droplet of mass  $s_1 \leq s - s_0$ , which occurs with probability  $\Omega_1 (s_1^{1/D} + s_0^{1/D})^d$ ,  $\Omega_1$  being a mass-independent geometric factor. The droplet of mass  $s_1$  consequently reaches a mass  $s_1 + s_0$ . Then it coalesces with a neighboring droplet of mass  $s_2 = s - s_1 - s_0$  provided that they interpenetrate. The number of such events is

$$\Omega_1 \Omega_2 N(s_1) N(s_2) (s_1^{1/D} + s_0^{1/D})^d \int_0^{(s_1+s_0)^{1/D} - s_1^{1/D}} G(s_1, s_2, r, t) (s_1^{1/D} + s_2^{1/D} + r)^{d-1} dr \quad (2.5)$$

( $\Omega_2$  is another geometric factor).  $G(s_1, s_2, r, t)$  is the probability density that a given droplet of mass  $s_1$  has a droplet of mass  $s_2$  at distance  $s_1^{1/D} + s_2^{1/D} + r$  as the first neighbor.

(ii) A droplet of mass  $s_0$  falls on a droplet of mass  $s - s_0$  with which it coalesces and the obtained droplet does not overlap any other droplet,

$$\begin{aligned} \text{(number of events)} &= \Omega_1 N(s - s_0) [(s - s_0)^{1/D} + s_0^{1/D}]^d \\ &\times \left( 1 - \Omega_2 \sum_{s_1 = k_1 s_0} N(s_1) \int_0^{s_1^{1/D} - (s - s_0)^{1/D}} G(s - s_0, s_1, r, t) [(s - s_0)^{1/D} + s_1^{1/D} + r]^{d-1} dr \right). \end{aligned} \quad (2.6)$$

(iii) A droplet falls in an empty space between droplets

$$(\text{number of events}) \propto [1 - \phi(t)] \delta_{s,s_0}, \tag{2.7}$$

where  $[1 - \phi(t)]$  is the empty area fraction.

A droplet of radius  $s$  disappears due to the following events: it coalesces with a droplet of radius  $s_1 + s_0$ , which has grown

$$(\text{number of events}) = \Omega_1 \Omega_2 N(s) N(s_1) (s_1^{1/D} + s_0^{1/D})^d \int_0^{(s_1+s_0)^{1/D} - s_1^{1/D}} G(s_1, s, r, t) (s_1^{1/D} + s_0^{1/D} + r)^{d-1} dr; \tag{2.8}$$

or it grows

$$(\text{number of events}) \propto N(s) (s^{1/D} + s_0^{1/D})^d. \tag{2.9}$$

To describe the long-time scaling regime, we can take the continuous limit of small (but finite)  $s_0$ , to obtain the continuous kinetic equation

$$\partial_t N(s, t) + \partial_s [s^{d/D} N(s, t)] = \frac{1}{2} \int_0^s N(s_1, t) N(s - s_1, t) K(s_1, s - s_1, t) ds_1, \tag{2.10}$$

$$- N(s, t) \int_0^{+\infty} N(s_1, t) K(s, s_1, t) ds_1 + I(t) \delta(s - s_0), \tag{2.11}$$

where the symmetric kernel  $K(x, y, t)$  is

$$K(x, y, t) = \lim_{\varepsilon \rightarrow 0} x^{d/D} / \varepsilon \int_0^{(x+\varepsilon)^{1/D} - x^{1/D}} G(x, y, r, t) (x^{1/D} + y^{1/D} + r)^{d-1} dr + (\text{symmetric terms}). \tag{2.12}$$

The time and mass units were redefined to eliminate multiplicative constants in the equation.  $I(t)$  is consequently renormalized to  $I(t) = c[1 - \phi(t)]$ , where  $c$  is a constant that could be easily determined, but is not essential to our discussion. It should be noticed that the distribution function is zero below  $s_0$  at any  $t$ .

The mean-field approximation consists in neglecting spatial correlations, i.e., in taking  $G(x, y, r, t) = 1$ . We get

$$K(x, y, t) = (x^{(d+1)/D-1} + y^{(d+1)/D-1}) (x^{1/D} + y^{1/D})^{d-1}. \tag{2.13}$$

This kernel has the homogeneity  $\lambda = 2d/D - 1$  derived from scaling arguments by Family and Meakin [9]. Equation (2.10) is not a standard Smoluchowski equation since it includes two additional terms: an *exogenous growth* term  $\partial_s [s^{d/D} N(s, t)]$ , describing intercollision growth of droplets through absorption of small droplets, and a time-dependent *injection* term. Moreover, the injection term is *self-consistent*: Being proportional to the free surface fraction, it is a functional of  $N(s, t)$  (see Sec. III D).

For the numerical model,  $I(t)$  vanishes at long times since the surface fraction covered by droplets goes to one in homogeneous growth processes, through renucleation in empty spaces (in heterogeneous nucleation models, the coverage goes to a value  $\bar{\phi} < 1$ ). In fact, our numerical simulations in one dimension show that in the scaling regime  $1 - \phi(t) \propto n(t)$ , as illustrated in Fig. 2. This result is easily recovered from the scaling theory,

$$1 - \phi(t) = 1 - \Omega S(t)^{1+d/D-\theta} \int_{s_0/S(t)}^{+\infty} x^{d/D} f(x) dx, \tag{2.14}$$

where  $\Omega$  is a geometric constant factor, which implies, since  $\phi(t) \rightarrow 1$  and  $\theta = 1 + d/D$ , that  $\int_0^{+\infty} x^{d/D} f(x) = \Omega^{-1}$ . Since  $f(x) \propto x^{-\tau}$ , we see that  $1 - \phi(t) \propto [s_0/S(t)]^{1+d/D-\tau}$  if  $\tau > 1$  and  $1 - \phi(t) \propto [s_0/S(t)]^{d/D}$  if  $\tau < 1$ , which yields  $1 - \phi(t)$

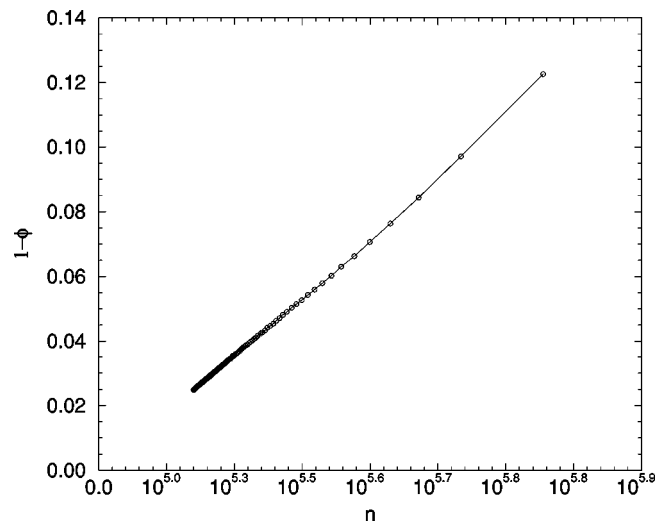


FIG. 2. Plot of the free substrate area  $1 - \phi(t)$  versus the number of droplets  $n(t)$  for a simulation of homogeneous growth with  $d=1$  and  $D=3$ . At long times (small  $n$ ), the two quantities are proportional, as understood in the framework of the scaling theory.

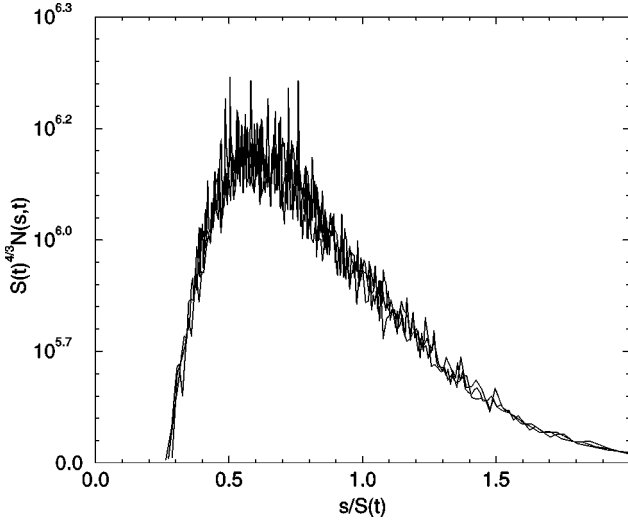


FIG. 3. Typical scaling function for heterogeneous nucleation with  $d < D$ . The figure shows the data collapse of  $N(s,t)$  in a simulation of growth and coalescence with  $\omega = -1$ ,  $d = 2$ , and  $D = 3$ . The scaling function is clearly monodisperse and vanishes at  $x_0 \approx 0.2$ .

$\propto n(t)$ . It is not obvious *a priori* that the dynamics of Eq. (2.10) will also lead to the vanishing of  $I(t)$  since geometrical constraints are only approximately included. This point will be discussed in Sec. III.

### B. Heterogeneous nucleation

Heterogeneous nucleation [5] corresponds to the case, common for water vapor condensation, when impurities on the substrate play a major role in droplet nucleation. A daily life example would be water condensation on a dusty pane. Nucleation occurs only on some nucleation centers, existing droplets grow from vapor, and coalesce when coming into contact, but no new droplet can nucleate in empty spaces.

In the *growth and coalescence* model introduced by Family and Meakin [9], one starts from an initial population of droplets of same radius without overlap. In the dynamics, individual droplets grow between collisions with

$$\dot{r} = Ar^\omega \quad (2.15)$$

or, equivalently ( $s = r^D$ ),

$$\dot{s} = DAs^\beta, \quad (2.16)$$

where  $\beta = (\omega + D - 1)/D$  and  $A$  is constant. Equation (2.15) has been known as type-I growth since the important theoretical work of Briscoe and Galvin [12] and is relevant to physical systems for which mass and/or heat transfer processes on the substrate are limited. In the following theoretical discussion we shall always set  $A = 1/D$ , but in numerical simulations  $A$  was set to 1 (this just corresponds to a change in the time unit). We must have  $\omega \leq 1$  (or, equivalently,  $\beta \leq 1$ ); otherwise the system gels as the mass of an individual droplet growing without collision diverges at finite time. One step of simulation consists in increasing the radii of all droplets according to a discretization of Eq. (2.15) and then track-

ing down and resolving all the resulting coalescence events, with the same rules as for homogeneous nucleation.

Droplets configurations obtained with this model for  $d < D$  and various values of  $\omega$  are qualitatively very different from those obtained with the deposition and coalescence model: there is now a single population of droplets with a bell-shaped mass distribution [9], as shown on Fig. 3 from simulations with  $d = 2$ ,  $D = 3$ , and  $\omega = -1$ . As in deposition and coalescence, an asymptotic scaling regime is reached at long times and the theoretical value  $\bar{\phi} = 1 + d/D$  can be derived from the fact that the surface coverage tends to a constant  $\bar{\phi}$ .

A distinctive feature of heterogeneous growth is that  $\bar{\phi} < 1$  (see [7,9] and references in [5]) and does not significantly depend on  $\omega$ . The value of the asymptotic coverage was computed by Derrida *et al.* [11] for several simplified models of coalescence in one dimension. Vincent [7] derived  $\bar{\phi} = 0.57$  from an approximate log-normal scaling solution to a Smoluchowski mean-field equation (see below) with four-body collisions included for  $d = 2$ ,  $D = 3$ , and  $\omega = -2$ , in excellent agreement with the numerical value  $\bar{\phi} = 0.55$ .

The exponent  $z$  can be *heuristically* determined from the fact that  $S(t)$  is the only mass scale in the asymptotic regime, which implies that the distance between droplets  $n^{1/d}$  scales as  $S^{1/D}$ . Then, from a rough evaluation of the total collision rate, it is justified in [5] that the growth law of the typical droplet mass in the asymptotic regime is the same as that of an individual droplet in the absence of collision, except for a multiplicative constant renormalizing the growth rate

$$\dot{S} \propto S^\beta, \quad (2.17)$$

which leads to

$$z = \frac{1}{1-\beta} = \frac{D}{1-\omega}. \quad (2.18)$$

These scaling results will be established for the corresponding Smoluchowski equation in Sec. III.

A consequence of Eq. (2.18) is that the scaling function  $f(x)$  cannot diverge at small  $x$  since a simple argument shows that  $f(x)$  is strictly zero below a finite  $x_0 > 0$ , as can be seen in Fig. 3 (see also Fig. 2 in [11]). Consider the smallest droplets surviving at  $t$ . These are the descendants of the droplets in the initial condition that have not experienced any collision since  $t = 0$ . As a consequence, the mass of the smallest surviving droplets  $s_0(t)$  is, for a strictly monodisperse initial condition  $N(s,0) \propto \delta(s - s_0)$ ,

$$s_0(t) \propto [s_0(0)^{1-\beta} + (1-\beta)t]^{1/(1-\beta)} \quad (2.19)$$

and  $s_0(t)/S(t)$  approaches a constant value  $x_0 > 0$ , independent of  $s_0(0)$ , when  $t \rightarrow \infty$ . Since  $N(s,t) = 0$  for  $s < s_0(t)$ , we see that  $f(x) = 0$  for  $x < x_0$ . For  $d = 2$ ,  $D = 3$ , and  $\omega = -1$ , our numerical results yield  $S(t) \sim 16 t^{1/(1-\beta)}$ , with  $\beta = 1/3$ , whereas  $s_0(t) \sim [(1-\beta)Dt]^{1/(1-\beta)}$  from Eq. (2.19) ( $D$  appears in the formula since  $A = 1$  in the simulation), which leads to  $x_0 \approx 0.2$ . This value of  $x_0$  is fully consistent with Fig. 3.

If  $\beta = 1$ , the growth of  $s_0(t)$  is exponential in time and the situation can be different. The collisions renormalize the growth of  $S(t)$  and we expect at long times

$$\dot{S} \sim [1 + \epsilon(t)]S(t), \quad (2.20)$$

where  $\epsilon$  is strictly positive. Even when  $\epsilon(t)$  asymptotically vanishes,  $S(t)$  can be much bigger than  $s_0(t)$ , leading to  $x_0 = 0$  and a possibly polydisperse distribution. This behavior will be found in Sec. III for the corresponding Smoluchowski equation. We shall see that  $S(t)$  is also much bigger than  $s_0(t)$  in the mean field in the case  $d = D$ , even for  $\beta < 1$ , as  $S(t) \propto (t \ln t)^{1/(1-\beta)}$ , and that polydispersity can occur in this case. Indeed, Family and Meakin [9] observed a qualitatively different, broader mass distribution, with polydispersity, in numerical simulations for  $d = D$ . This case will be further investigated in Sec. IV.

Now we proceed in deriving Smoluchowski's equation for this problem. If we assume that droplets do not coalesce, we can find the contribution to Smoluchowski's equation due to the growth of individual droplets. The corresponding term must conserve the number of particle since no new droplet is introduced in the system and the equation is just a continuity equation for the distribution function  $N(s, t)$ ,

$$\partial_t N(s, t) + \partial_s (s^\beta N)(s, t) = 0. \quad (2.21)$$

If we bring coalescence into the picture, the rate of coalescence of two droplets of masses  $s_1$  and  $s_2$  is, under the mean-field assumption, the time derivative of the overlap probability proportional to  $(s_1^{1/D} + s_2^{1/D})^d$ , which is proportional to  $(s_1^{1/D-1} \dot{s}_1 + s_2^{1/D-1} \dot{s}_2)(s_1^{1/D} + s_2^{1/D})^{d-1}$ . So eventually

$$\begin{aligned} \partial_t N(s, t) + \partial_s (s^\beta N)(s, t) \\ = \frac{1}{2} \int_0^s N(s_1, t) N(s - s_1, t) K(s_1, s - s_1) ds_1 \\ - N(s, t) \int_0^{+\infty} N(s_1, t) K(s, s_1) ds_1, \end{aligned} \quad (2.22)$$

with

$$K(x, y) = (x^{\omega/D} + y^{\omega/D})(x^{1/D} + y^{1/D})^{d-1}. \quad (2.23)$$

Once again, redefinition of the time and mass unit was used to set multiplicative constants to one in the equation.

Here we would like to point out a mistake in an early numerical and theoretical work by Vincent [7]. Vincent studied heterogeneous growth with  $d = 2$ ,  $D = 3$ , and  $\omega = -1$ , relevant to epitaxial growth. He simulated early stages of growth (because he could not reach the long-time asymptotic regime) and derived a mean-field Smoluchowski equation for the radius distribution  $\psi(r, t) = D r^{1-1/D} N(r^D, t)$ . Vincent found the correct collision kernel, but he erroneously derived that the change in  $\psi$  due to growth alone was  $-r^{-2} \partial_r \psi$ , instead of the correct  $-\partial_r (r^{-2} \psi)$ . As a consequence, his equation does not conserve the number of particles when the collision term is suppressed. This might be one of the reasons why Vincent had to include three- and four-body coalescence events in his Smoluchowski equation to recover

correct values for the fraction of area covered by the droplets, but the incorrect right-hand side may as well have only minor consequences in his approximate computation.

An interesting case arises when  $\omega = 1 + d - D$  since, as noticed by Family and Meakin [9], this corresponds to the growth exponent of large droplets due to absorption of deposited small droplets in homogeneous growth. In this case, Smoluchowski's equation describing homogeneous growth differs from the one describing heterogeneous growth only by the injection term. Exponents  $\theta$  and  $z$  are the same for both models and numerical simulations [9,5] show that the scaling function for large droplets in homogeneous growth is very similar to the whole scaling function of heterogeneous growth.

Thus both growth and coalescence, and deposition and coalescence, are described in the mean field by a generalized Smoluchowski equation, with additional terms accounting for intercollision exogenous growth of particles (droplets). Therefore, it is interesting to perform a general study of this equation (with a generic kernel) and to see if its scaling behavior is consistent with the numerical results for droplets nucleation.

### III. SMOLUCHOWSKI'S EQUATION WITH GROWTH AND INJECTION

We consider the generalized Smoluchowski equation

$$\begin{aligned} \partial_t N(s, t) + \partial_s [s^\beta N(s, t)] \\ = \frac{1}{2} \int N(s_1, t) N(s - s_1, t) K(s_1, s - s_1) ds_1 \\ - N(s, t) \int N(s_1, t) K(s, s_1) ds_1 + I(t) \delta(s - 1), \end{aligned} \quad (3.1)$$

$K(x, y)$  being a general homogeneous kernel with exponents  $\lambda$  and  $\mu$  defined as in Eq. (1.2). The equation describes a set of particles or clusters that collide with a mass-dependent collision rate  $K$  and grow between collisions with (see below)

$$\dot{s} = s^\beta. \quad (3.2)$$

In addition, some small particles (monomers) are injected with the injection rate  $I(t)$ , with the possibility that  $I$  is a functional of  $N(s, t)$ , as found for deposition and coalescence in Sec. II. A discrete version of this equation without the monomer injection term and with a *constant collision kernel* has been investigated for  $0 \leq \beta \leq 1$  by Krapivsky and Redner [22]. We shall see below that their results are independently recovered as special cases of our general discussion of the continuous equation, in the scaling regime where the discrete structure of the equation plays no role.

When the growth and injection terms are absent, the equation reduces to Smoluchowski's equation and its scaling properties have been extensively studied [18–20], but it is in no way trivial. Even in this case, very few analytical solutions of Smoluchowski's equation are available. For the constant kernel  $K(x, y) = 1$ , an exact solution is known [16],

with  $N(s,t) \sim 4/t^2 e^{-2s/t}$ . Other solutions concern the kernels  $x+y$  [23] and  $xy$  [24]. Despite its apparently simple structure, Smoluchowski's equation is yet another example of a highly nontrivial mean-field theory.

In the following we study the long-time properties of the solutions of Eq. (3.1) and we exhibit a rich diversity of behaviors depending on the parameters  $\beta$  (characteristic of exogenous growth) and  $\lambda$  and  $\mu$  (characteristic of the collision kernel). We use the classical notation  $M_\alpha(t)$  for the  $\alpha$ th moment of the distribution  $\int s^\alpha N(s,t) ds$ .

### A. Gelation criterion

The first interesting question is the possible occurrence of a gelation transition for such equations. Gelation corresponds to the formation of an infinite cluster *at finite time*. Without a growth term, nongelling kernels correspond to  $\lambda \leq 1$  [18,19]. How is this modified? In the absence of an infinite cluster, the evolution equation for the total mass in the system  $M_1(t)$  is obtained by multiplying Smoluchowski equation by  $s$  and integrating over all masses,

$$\dot{M}_1(t) = M_\beta(t) + I(t), \quad (3.3)$$

which is physically obvious from  $\dot{s} = s^\beta$ . To discuss gelation, we have to be more cautious. Adapting the argument for the standard Smoluchowski equation [25,26,18,19], let us consider the mass flux from clusters of masses  $s \leq L$  towards clusters of masses  $s > L$ ,

$$J_L(t) = - \int_0^L s \partial_t N(s,t) ds + \int_0^L \dot{s} N(s,t) ds + I. \quad (3.4)$$

From Eq. (3.1) we get

$$J_L(t) = L^{1+\beta} N(L,t) + \int_0^L dx x N(x,t) \int_{L-x}^{+\infty} dy K(x,y) N(y,t), \quad (3.5)$$

where the first term is the mass flux through  $s=L$  due to the growth of individual particles, while the second term is the mass flux due to collisions. If there is no gelation  $J_L(t)$  must vanish when  $L \rightarrow \infty$  and Eq. (3.3) holds at any time. If there is gelation at  $t=t_g$ , there is an infinite cluster, or gel, in the system for  $t > t_g$  and  $J_L(t)$  is nonvanishing for  $t > t_g$ . At the gel point,  $J_\infty(t) = \lim_{L \rightarrow \infty} J_L(t)$  may be infinite, but not for  $t > t_g$ . The postgel distribution must have a slowly decaying large- $s$  tail in order that  $J_\infty(t)$  be finite. If we make the ansatz  $N(s, t \geq t_g) \sim A(t) s^{-\tau}$  at large  $s$ ,

$$L^{1+\beta} N(L,t) \sim A(t) L^{1+\beta-\tau}, \quad (3.6)$$

$$\begin{aligned} & \int_0^L dx x N(x,t) \int_{L-x}^{+\infty} dy K(x,y) N(y,t) \\ & \sim A(t)^2 L^{3+\lambda-2\tau} \int_0^1 dx \int_{1-x}^{+\infty} dy x K(x,y) (xy)^{-\tau}. \end{aligned} \quad (3.7)$$

We see that if gelation occurs,  $\tau$  must be equal to  $\max[1+\beta, (3+\lambda)/2]$ . In the postgel regime, the total mass

contained in the sol phase (i.e., finite mass clusters) must be finite, which imposes  $\tau > 2$ . We conclude that no gelation occurs for  $\max(\lambda, \beta) \leq 1$ . In any case,  $\beta > 1$  is forbidden since it leads to explosive growth of individual particles. If  $\beta = 1$ , Eq. (3.3) yields  $M_1(t) = e^t$  and the total mass growth is faster than any power of  $t$ , which is the telltale of the gelling-nongelling boundary.

### B. No injection

For a while, we specialize to the case  $I=0$ , corresponding to growth and coalescence. We first exhibit two exact solutions and then we make a complete study of the scaling solutions of the general equation.

#### 1. Exact solutions

We can solve Eq. (3.1), in the case  $K(x,y)=1$ , for  $\beta=0$  and  $\beta=1$ . To do this, we consider the Laplace transform  $Z(z,t)$  of  $N(s,t)$ ,  $Z(z,t) = \int_0^{+\infty} e^{-zs} N(s,t) ds$ .  $Z(0,t)$  is the total density of clusters  $n(t)$ .

For  $\beta=0$ , the Laplace transform of Eq. (3.1) with  $K=1$  reads

$$\partial_t Z + zZ = \frac{1}{2} Z^2 - Z(0,t)Z. \quad (3.8)$$

With  $n(0)=1$  and  $Z(z,0)=Z_0(z)$ , we find that  $Z(0,t) = n(t) = 2/(t+2)$  and

$$Z(z,t) = \frac{e^{-zt}}{(t+2)^2 \left( \frac{1}{4Z_0(z)} - \frac{1}{2} \int_0^t \frac{e^{zt'}}{(t'+2)^2} dt' \right)}. \quad (3.9)$$

For a strictly monodisperse initial condition  $N(s,t) = \delta(s-1)$ , the total mass in the system is  $M_1(t) = -\partial_z Z(z=0,t) = 1 + 2 \ln(t + \frac{1}{2})$  and in the scaling limit  $t \rightarrow \infty$ ,

$$N(s,t) \sim \frac{2}{t^2 \ln t} e^{-s/(t \ln t)}. \quad (3.10)$$

For  $\beta=1$ , the equation for  $Z$  is

$$\partial_t Z - z \partial_z Z = \frac{1}{2} Z^2 - Z(0,t)Z \quad (3.11)$$

and once again  $n(t) = Z(0,t) = 2/(t+2)$ . If we choose the variable  $u = ze^t$ , the equation reduces to a first-order differential equation in time and the solution is

$$Z(z,t) = \frac{2}{t+2} \frac{2Z_0(ze^t)}{[1 - Z_0(ze^t)](t+2) + 2Z_0(ze^t)}. \quad (3.12)$$

With a strictly monodisperse initial distribution,  $Z_0(z) = e^{-z}$ ,  $Z(z,t)$  has a pole at  $z_0(t) = -e^{-t} \ln(1+2/t)$ , and we can explicitly compute  $N(s,t)$ ,

$$N(s,t) = \frac{4}{(t+2)^2 e^t} \exp[-se^{-t} \ln(1+2/t)], \quad (3.13)$$

which leads in the long-time limit to

$$N(s,t) \sim \frac{4}{t^2} e^{-2s/te^t}. \quad (3.14)$$

Thus both solutions exhibit dynamic scaling. The corresponding solutions for the discrete Smoluchowski equation have been derived independently by Krapivsky and Redner [22] and coincide with the solutions above in the scaling limit. This coincidence was to be expected since, in the scaling regime, the divergence of  $S(t)$  leads to the oblivion of the discrete structure of the equation. The scaling function is the same as for the exact solution of  $K=1$  without exogenous growth, but instead of the usual scaling relation of Eq. (2.1), we have  $N(s,t) \sim Y(t)^{-1} f(s/S(t))$ , where  $Y(t) \propto S^2(t)/M_1(t)$  is not a power of  $S(t)$ .

A consequence of the logarithmic correction in the case  $\beta=0$  is that in contrast to the generic case in Sec. II B,  $x_0$  is equal to zero. The reason is that  $S(t)$  in this case grows faster than individual particles in the absence of collisions. Hence  $s_0(t)/S(t) \propto 1/\ln t$  goes to zero. This point will be fully discussed in the case of a general kernel under the dynamic scaling assumption. For  $\beta=1$ , the scenario discussed in Sec. II B occurs and  $S(t) \sim te^t$  corresponds to a slowly vanishing  $\epsilon(t)$  in Eq. (2.20).

## 2. Scaling theory

In the general case, Eq. (3.1) can be neither solved analytically nor easily simulated. However, some very interesting information can be obtained by making use of the scaling assumption. Note that, although it is quite clear from their homogeneity that Smoluchowski-like equations admit scaling solutions, it has never been mathematically proved that these solutions are approached at long times, except in the few cases for which we can obtain the exact solution. However, scaling is commonly observed experimentally and numerically for aggregation models, as well as in numerical solutions of Smoluchowski's equation [27] when possible, making this assumption very reasonable.

Some simple arguments may give a qualitative understanding of the different regimes to be expected for Eq. (3.1). Indeed, if we suppress the collision term (i.e., the right-hand side), we are left with a continuity equation that describes a set of particles that grow in time with  $\dot{s} = s^\beta$  and is associated with the mass scale  $S_g(t) \propto t^{1/(1-\beta)}$ .

Conversely, if we suppress the exogenous growth term  $\partial_s(s^\beta N)$  on the left-hand side, we have again a standard Smoluchowski equation describing clustering with mass conservation. The scaling properties of this equation are well known [18–20]. The typical mass in the scaling regime is  $S_c(t) \propto t^{1/(1-\lambda)}$  and  $\theta=2$ .

Thus, when both exogenous growth and collisions are active, we expect to observe a ‘‘competition’’ between the two dynamical mass scales  $S_c$  and  $S_g$ . If  $\beta > \lambda$ ,  $S_g(t) \gg S_c(t)$  and in the scaling regime we expect  $S(t) \propto S_g(t)$  and  $z = 1/(1-\beta)$ . If  $\beta < \lambda$ , on the contrary, the typical mass of particles increases essentially due to collisions, hence  $S(t) \propto t^{1/(1-\lambda)}$  and  $z = 1/(1-\lambda)$ . In the marginal case  $\lambda = \beta$ , logarithmic corrections to  $S(t)$  may be observed. In fact, we know from the exact solution of  $K=1$ ,  $\beta=0=\lambda$  that such corrections

actually occur. This leads us to a slightly more general scaling assumption than the one we made for droplets coalescence models,

$$N(s,t) \sim Y(t)^{-1} f\left(\frac{s}{S(t)}\right). \quad (3.15)$$

We do not *a priori* assume that  $Y(t) \propto S(t)^\theta$  since we know from exact solutions that it is not always true.

Notice that the scaling function  $f(x)$  is not uniquely defined by Eq. (3.15) unless we give a precise definition of  $S(t)$  and  $Y(t)$ . If we know a scaling function  $f_s(x)$  for given definitions of  $Y$  and  $S$ , any other scaling function  $f(x)$  corresponding to other definitions is related to  $f_s$  by

$$f(x) = \kappa f_s(\xi x), \quad (3.16)$$

$\kappa$  and  $\xi$  being two constants. The most usual definition of  $S(t)$  (and the one actually used in numerical simulations) is Eq. (2.2).

From the picture above, it is obvious that the physical cutoff, i.e., the mass  $s_0(t)$  below which  $N(s,t)$  is strictly zero, scales as  $S_g(t)$ . This is just the translation, in terms of Smoluchowski's equation, of the discussion we had for droplet growth and coalescence. Since  $S(t) \geq s_0(t)$ , either  $S(t)$  and  $S_g(t)$  have the same scaling and the scaling function  $f(x)$  is zero below a certain argument  $x_0 > 0$  or  $S(t) \gg S_g(t)$ ,  $x_0$  is equal to zero, and  $f$  may have a small  $x$  divergence  $f(x) \propto x^{-\tau}$ , with a polydispersity exponent  $\tau \geq 0$ .

The scaling of the moments of the distribution  $N(s,t)$  is altered by the existence of a polydispersity exponent

$$M_\alpha = \int_{s_0(t)}^{+\infty} s^\alpha N(s,t) ds \sim \frac{S^{1+\alpha}}{Y} \int_{s_0(t)/S(t)}^{+\infty} x^\alpha f(x) dx. \quad (3.17)$$

If there is no polydispersity exponent or if  $\tau < 1 + \alpha$ , the integral tends to a finite limit when  $t \rightarrow \infty$  and

$$M_\alpha(t) \propto \frac{S^{1+\alpha}}{Y}. \quad (3.18)$$

If  $\tau > 1 + \alpha$ , the integral diverges and

$$M_\alpha(t) \propto \frac{S^\tau}{Y} s_0(t)^{1+\alpha-\tau}. \quad (3.19)$$

Finally, if  $\tau = 1 + \alpha$ ,

$$M_\alpha(t) \propto \frac{S^{1+\alpha}}{Y} \ln \frac{S(t)}{s_0(t)}. \quad (3.20)$$

Under the general scaling assumption, we get the following scaling for the different terms of Smoluchowski's equation:

$$\partial_t N(s,t) \sim -\frac{1}{Y} \left( \dot{Y} f(x) + \dot{S} x f'(x) \right), \quad (3.21)$$

$$\partial_s [s^\beta N(s,t)] \sim \frac{S^{\beta-1}}{Y} (x^\beta f)'(x), \quad (3.22)$$

$$(\text{collision term}) \sim \frac{S^{1+\lambda}}{Y^2} (\dots). \quad (3.23)$$



TABLE I. Results of the scaling theory.

Parameters	$M_1(t)$	$S(t)$	$Y(t)$
$1 > \beta > \lambda$	$M_1 \propto S^{\beta-\lambda}$	$S(t) \propto t^z$ $z = \frac{1}{1-\beta}$	$Y \propto S^\theta$ $\theta = 2 + \lambda - \beta$
$1 > \lambda > \beta$	$M_1 \rightarrow \text{const}$	$z = \frac{1}{1-\lambda}$	$\theta = 2$
$1 > \lambda = \beta$	$M_1 \propto \begin{cases} \ln t & \text{if } \mu \leq 0 \\ (\ln t) \ln(\ln t) & \text{if } \mu > 0 \end{cases}$	$S(t) \propto (t M_1)^z$ $z = \frac{1}{1-\beta}$	$Y \propto \frac{S^2}{M_1}$
$\beta = 1$ $0 < \lambda < 1$	$M_1 = M_1(0) e^t$	$S(t) \propto e^{t/(1-\lambda)}$	$Y \propto S^2 e^{-t}$
$\beta = 1$ $\lambda = 0$	$M_1 = M_1(0) e^t$	$S(t) \propto t e^t$	$Y \propto t S$
$\lambda = 1 > \beta$ $\mu > 0$	$M_1 \rightarrow \text{const}$	$S(t) \propto e^{b\sqrt{t}}$	$Y \propto S^2 \sqrt{t}$
$\lambda = 1 > \beta$ $\mu \leq 0$	$M_1 \rightarrow \text{const}$	$S(t) \propto e^{bt}$	$Y \propto S^2$
$\lambda = \beta = 1$ $\mu \leq 0$	$M_1 = M_1(0) e^t$	$S(t) \propto e^{be^t}$	$Y \propto S^2 e^{-t}$
$\lambda = \beta = 1$ $\mu \leq 0$	$M_1 = M_1(0) e^t$	$S(t) \propto e^{b\sqrt{e^t}}$	$Y \propto S^2 e^{-t/2}$

Another important equation is Eq. (3.3) for the evolution of the total mass in the system, which, in the absence of injection, reduces to

$$\dot{M}_1 = M_\beta. \quad (3.24)$$

Now it is possible to find the asymptotics of  $M_1$ ,  $Y$ , and  $S$ , depending on the values of  $\lambda$  and  $\beta$ , under the sole scaling assumption. In fact, although the line followed in the demonstration is quite simple, details are rather intricate due to the multiple cases to be examined. A full length discussion is given in the Appendix and results are summarized in Table I. Here we shall only comment on some interesting points.

The scaling theory is consistent with the qualitative discussion above based on the idea of competing dynamical scales. It is found that for  $\lambda < \beta < 1$ ,  $S(t)$  scales as  $s_0(t) \sim t^{1/(1-\beta)}$ ,  $Y(t) \propto S(t)^{-\theta}$ , with  $\theta = 2 + \lambda - \beta$ , and the scaling function is zero below a finite  $x_0$ . If we return to droplets models, this  $\lambda < \beta$  condition just corresponds to  $d < D$  and we find  $\theta = 1 + d/D$ . Hence the scaling results of the mean-field theory are in full agreement with the discussion and results in Sec. II B.

For  $\lambda > \beta$ ,  $S(t)$  scales as  $t^{1/(1-\lambda)}$  and the mass is asymptotically conserved with  $\theta = 2$ . The scaling function may have a polydispersity exponent, since now  $S(t) \gg s_0(t)$ , and the scaling equation is,

$$b[xf'(x) + 2f(x)] = f(x) \int_0^{+\infty} f(x_1) K(x, x_1) dx_1 - \frac{1}{2} \int_0^x f(x_1) f(x-x_1) K(x_1, x-x_1) dx_1, \quad (3.25)$$

i.e., the same scaling equation as for the standard Smoluchowski equation without cluster exogenous growth, which makes it possible to use all the corresponding results or techniques [18–20]. For breath figures, this case corresponds to  $d > D$ , but as further discussed in Sec. IV, heterogeneous growth is always gelling in this case and the mean-field approximation breaks down.

For  $\lambda = \beta$ , we find that  $S(t)$  is no longer a pure power law, but incorporates logarithmic corrections. The total mass in the system increases logarithmically,  $M_1(t) \propto \ln t$  and  $S(t) \sim [t M_1(t)]^{1/(1-\beta)}$ . Once again  $S(t) \gg s_0(t)$  and the scaling function is Eq. (3.25). Thus there is a polydispersity exponent if the kernel has  $\mu \geq 0$  (see below) and there is an addition  $\ln(\ln t)$  correction for  $\mu > 0$  kernels. For heterogeneous growth,  $\lambda = \beta$  corresponds to  $d = D$  and the mean-field theory accounts for the qualitative difference between  $d = D$  and  $d < D$  observed in numerics (see [9] and below). This point will be fully discussed in Sec. IV. This also recovers the scaling behavior of the exact solution for  $K = 1$  and  $\beta = 0$ .

For  $\beta = 1$ , the scaling of the exact solution  $K = 1$ ,  $\beta = 1$  is recovered. For  $\lambda \geq 0$ , the scaling equation is once again Eq. (3.25). Other results in Table I show the great diversity of scaling regimes depending on  $\beta$ ,  $\lambda$ , and  $\mu$ .

For a constant kernel and  $1 > \beta > 0$ , we recover the result of Krapivsky and Redner [22], who assumed that the scaling function has essentially the same shape as in the case  $\beta = 0$  or the pure aggregation case. From our analysis, we know that this assumption is actually not verified. However, it can be seen that the key point of their demonstration is that  $f(x)$  has no small- $x$  divergence, which is indeed true.

The fact that the scaling results of the  $d < D$  growth and coalescence are recovered by the Smoluchowski equation approach gives a firm basis to the heuristic arguments used to

find *a posteriori* the exponents from the obtained numerics. Moreover, the kinetic equation approach is predictive and provides a synthesized classification of the aggregation models, depending on a limited number of relevant parameters, provided the approximation is justified.

### 3. Polydispersity exponents

An interesting corollary of the scaling theory of the generalized Smoluchowski equation with growth is that in the cases  $\beta \leq \lambda$  and  $\beta = 1$ , the scaling equation is exactly the same as for the standard Smoluchowski equation (3.25), where  $b$  is called the separation constant, which we set to one by absorbing it in the scaling function (which corresponds to a redefinition of  $Y$ ). Note that if  $f$  is a solution of Eq. (3.25),  $c^{1+\lambda}f(cs)$  is also a solution, which corresponds to different possible definitions of  $S(t)$  [remember the discussion above Eq. (3.16)].

Thus all the results known for the scaling function of the standard Smoluchowski equation also hold for the generalized equation. For instance, the scaling function  $f(x)$  of the  $K=1, \beta=1$  case can be derived from the exact result for the standard Smoluchowski equation with  $K=1$ , for which  $f_0(x) = e^{-x}$  is a scaling function. For a given definition of  $S$  and  $Y$ , the corresponding scaling function for  $K=1, \beta=1$  is obtained using  $f_s = f_0$  in Eq. (3.16). If we use Eq. (2.2) as a definition of  $S(t)$ ,  $\xi$  is constrained to the value  $\xi=2$ ; if we define  $Y(t)$  by  $M_1(t) = S^2/Y$ , we get  $\kappa=4$ , which leads to

$$N(s,t) \propto \frac{4e^t}{S^2} e^{-2s/S}, \quad (3.26)$$

with  $S(t) \propto te^t$  in agreement with the exact result Eq. (3.14).

We can also find the exact scaling function for  $\beta=1$  and  $K(x,y) = x+y$  (which corresponds to  $\lambda=1$ ). For the standard Smoluchowski equation, a scaling function is  $f_1(x) = x^{-3/2}e^{-x}$ . It is also a scaling function for Eq. (3.1) and we obtain the exact result  $\tau=3/2$ .

The scaling equation (3.25) for a general kernel was extensively studied in the literature. van Dongen and Ernst [18,19] showed that the qualitative shape of the scaling function  $f(x)$  at small  $x$  depends on two parameters: the homogeneity degree of the kernel  $\lambda$  and the exponent  $\mu$  defined by Eq. (1.2).

For  $\mu < 0$ , the scaling function vanishes as  $\exp[-\alpha x^\mu + o(x^\mu)]$  at small  $x$  and there is no polydispersity exponent. For kernels with  $\mu > 0$ , there is a polydispersity exponent  $\tau = 1 + \lambda$ . For  $\mu = 0$ , there is also polydispersity, but with a nontrivial exponent  $\tau < 1 + \lambda$ ,

$$\tau = 2 - \int_0^{+\infty} x^\lambda f(x) dx. \quad (3.27)$$

The determination of  $\tau$  for  $\mu=0$  has long been a challenge because solving numerically Smoluchowski's equation proved rather difficult and often unsuccessful. Even for the most studied  $\mu=0$  kernel

$$K_D^d(x,y) = (x^{1/D} + y^{1/D})^d, \quad (3.28)$$

which corresponds, for instance, to Brownian coalescence [in a  $(d+2)$ -dimensional space] with mass-independent diffusion constant, very few values of  $\tau$  were known.

This difficulty appears to be overcome by a *variational method*, which we have introduced in a recent paper [20]. A systematic computation of  $\tau$  can now be performed in a simple way at a very low numerical cost. We report such a computation for the kernel  $K_D^d$  in [20]. Analytical results combined with exact inequalities obtained from Eq. (4.7) are used to check the variational results, which are also in excellent agreement with the few values of  $\tau$  available in the literature.

From the discussion above, we see that the variational method can also be used to determine  $\tau$  for Smoluchowski's equation with exogenous growth of particles, when polydispersity occurs, i.e., when  $\lambda = \beta$  or  $\beta = 1$ . An interesting physical application of these results is *heterogeneous growth with  $d=D$* , which is in the class  $\beta = \lambda$ . For this problem,  $\beta$  is equal to  $1 + (\omega - 1)/D$  and the kernel is

$$K(x,y) = (x^{\omega/D} + y^{\omega/D})(x^{1/D} + y^{1/D})^{D-1}. \quad (3.29)$$

This kernel is formally similar to the one describing diffusion-limited cluster-cluster aggregation [14,15,28], but the meaning of the parameters is different. We have

$$\mu = \begin{cases} 0 & \text{if } \omega \geq 0 \\ \omega/D & \text{if } \omega < 0. \end{cases} \quad (3.30)$$

The scaling theory yields  $S(t) \propto (t \ln t)^z$ , with  $z = D/(1 - \omega)$ , and predicts a transition from a polydisperse scaling function with a nontrivial  $\tau$  exponent for  $\omega \geq 0$  to a small- $x$  vanishing scaling function for  $\omega < 0$ .

Consequently, it is interesting to determine the mean-field polydispersity exponent  $\tau$  for this kernel using the variational approximation. This will be done in Sec. IV, in which we also present comparisons of scaling results from the Smoluchowski equation approach with direct numerical simulations of heterogeneous growth with  $d=D$ .

### C. Constant injection

We now move to the case of a constant injection rate. Interest in aggregation models with injection was originally aroused from applications in chemical engineering (coagulation in stirred tank reactors) and atmosphere sciences [29–37]. In these contexts, injection was often associated with a sink term. The emergence of the concept of self-organized criticality [38,39] resulted in a renewal of interest in aggregation models with constant injection [40–42] since these systems commonly evolve to a steady-state asymptotic power-law distribution and therefore provide examples of self-organized critical systems. This behavior is assessed by numerical simulations and exact solutions in one dimension [41,42].

Hayakawa [37] studied Smoluchowski's equation with injection of a monomer. He showed that for nongelling systems, with  $\lambda < 1$  [18], the asymptotic steady state had a power-law large- $s$  decay with an exponent  $\tau = (3 + \lambda)/2$ . Here we shall investigate the steady state in the presence of a growth term with exponent  $\beta$ . We assume for convenience that the coagulation kernel  $K(x,y)$  is equal to  $x^\mu y^\nu + x^\nu y^\mu$ .

$\lambda = \mu + \nu$  is the homogeneity degree of the kernel. The results are true, however, for any kernel.

We are interested in the asymptotic steady state reached by the system at long times. We shall see that it has a large- $s$  power-law decay with an exponent  $\tau$  that we are able to compute in terms of  $\lambda$  and  $\beta$ . To achieve this program, let us call  $Z_\alpha(z, t)$  the Laplace transform of  $s^\alpha N(s, t)$  defined by

$$Z_\alpha(z, t) = \int_0^{+\infty} s^\alpha N(s, t) e^{-zs} ds, \quad (3.31)$$

for which we get

$$\partial_t Z_1 + z Z_\beta = Z_\mu Z_\nu - Z_\mu M_\nu - Z_\nu M_\mu + I e^{-z}. \quad (3.32)$$

Now we consider the equation for the steady state,

$$z Z_\beta^\infty = (Z_\mu^\infty - M_\mu^\infty)(Z_\nu^\infty - M_\nu^\infty) + I(e^{-z} - 1). \quad (3.33)$$

The large- $s$  behavior of the steady-state distribution is reflected in the small- $z$  behavior in Laplace space,

$$Z_\alpha^\infty(z) - M_\alpha^\infty \sim c_\alpha z^{\tau_\alpha} \quad (3.34)$$

if  $M_\alpha^\infty$  is finite. If  $M_\alpha^\infty$  is infinite, it does not appear on the left-hand side. Note that  $M_1^\infty$  is certainly infinite because there is constant injection of monomers and no dissipation of mass (at finite time). As a consequence,  $0 < \tau_\alpha < 1$  for all  $\alpha < 1$ . If  $\tau_\alpha$  is not an integer then for  $s \rightarrow \infty$ ,

$$s^\alpha N(s, t = \infty) \sim \frac{c_\alpha}{2\pi} \Gamma(1 + \tau_\alpha) s^{1 - \tau_\alpha}. \quad (3.35)$$

As a consequence,  $\tau - 1 = \tau_0 = \tau_\alpha + \alpha$  and

$$z(M_\beta + I + z^{\tau-1-\beta}) \propto (z^{2\tau-2-\lambda}); \quad (3.36)$$

hence if  $\tau - 1 - \beta > 0$ , then  $1 = 2\tau - 2 - \lambda$ , i.e.,  $\tau = (3 + \lambda)/2$ , whereas if  $\tau - 1 < \beta$ ,  $M_\beta^\infty$  is infinite and does not appear on the left-hand side of Eq. (3.36) and then  $\tau - \beta = 2\tau - 2 - \lambda$ , i.e.,  $\tau = 2 - \beta + \lambda$ . To summarize, we find

$$\tau = \begin{cases} (3 + \lambda)/2 & \text{if } \beta < (1 + \lambda)/2 \\ 2 + \lambda - \beta & \text{if } \beta > (1 + \lambda)/2. \end{cases} \quad (3.37)$$

Thus we see that the exogenous growth term introduces the following feature: Above a critical growth parameter  $\beta_c = (1 + \lambda)/2$ , the power-law exponent of the asymptotic state depends continuously on  $\beta$ , whereas if  $\beta$  is less than  $\beta_c$ , the exponent is unaffected by the growth term.

The case  $\beta = (1 + \lambda)/2$  requires some additional care. Interpolation of the two regimes above would lead to  $\tau = 1 + \beta$  and it is possible to show that there is a logarithmic correction  $N(s, +\infty) \propto 1/(s^{1+\beta} \ln s)$ .

For  $\beta < 1 + \lambda$ ,  $\tau$  has the value found by Hayakawa [37] in the absence of exogenous growth from the same Laplace transform arguments. It is also interesting to derive  $\tau$  from a more physical argument. For convenience, let us first forget the exogenous growth term (the argument is the same) and consider the steady-state condition.  $N_\infty(s)$  is a stationary distribution in the sense that if we start from  $N(s, t=0) = N_\infty(s)$ , then the distribution does not evolve. From this

point of view, it becomes clear that the total mass injection rate  $I$  must exactly be compensated by the mass dissipation by collisions. Thus the total mass flux due to collisions must be finite. This just means that the steady state is at a *gel point* and the argument of Sec. III A can be readily adapted to obtain  $\tau = (3 + \lambda)/2$ . Furthermore, as the total mass is infinite in the steady state, we do not have the restriction  $\tau > 2$ , which determines the gel criterion for gelation at a finite time. Here the transition occurs at an infinite time, when the system has self-organized to the critical point of a gel transition.

If we introduce the exogenous growth term into the picture, we can also find the exponents from the same argument. Now the mass injection rate is  $I + M_\beta^\infty$ . If  $M_\beta^\infty$  is finite, we still find  $\tau = (3 + \lambda)/2$ . If  $\beta \geq (1 + \lambda)/2$ ,  $M_\beta^\infty$  is diverging with such a value of  $\tau$ . Consequently,  $M_\beta^\infty$  is infinite and the steady-state condition is now

$$I + \lim_{L \rightarrow \infty} \left( \int_0^L s^\beta N_\infty(s) ds - C(L) \right) = 0, \quad (3.38)$$

where  $C(L)$  is the integral in Eq. (3.5). The vanishing of the divergence imposes  $1 + \beta - \tau = 3 + \lambda - 2\tau$  and we recover  $\tau = 2 + \lambda - \beta$ .

#### D. Constant mass injection

Now we would like to return to the initial problem of homogeneous nucleation and the corresponding Smoluchowski equation. The corresponding collision kernel has  $\lambda = 2d/D - 1 = 2\beta - 1$ , just on the borderline of the two regimes found for constant injection. The point we make is that injection of small droplets occurs at a vanishing rate proportional to  $1 - \phi(t)$ , as seen in Sec. II B from a geometrical interpretation. In fact, forgetting geometry,  $I(t)$  is imposed by the fact that the mass injection rate is a constant (by definition of the model), say,  $\dot{M}_1 = 1$ . Indeed, from  $\dot{M}_1 = M_\beta + I$ , this is equivalent to  $I(t) = 1 - M_\beta(t)$ . For droplet deposition and with this choice of constants,  $M_\beta(t) = \phi(t)$  and the geometrical argument is recovered.

Accordingly, we now discuss the case of  $\lambda = 2\beta - 1$  and constant mass injection  $\dot{M}_1 = 1$ , i.e.,

$$I(t) = 1 - M_\beta(t), \quad (3.39)$$

for  $\beta < 1$ . Once again, we make the scaling assumption of Eq. (3.15). As in homogeneous nucleation,  $M_1(t) \propto t$  leads to  $Y(t) \propto S^2/t$ . A very interesting result is that  $M_\beta$  must tend to 1 at long times. First, it is easily seen that  $M_\beta(t)$  cannot diverge. The reason is that the injection rate of ‘‘area’’ into existing particles is equal to  $\beta M_{2\beta-1}$  and is always dominated by  $M_\beta(t)$  in the scaling regime. More precisely, the evolution equation for the occupied area fraction  $M_\beta$  is obtained from Eq. (3.1) and since collisions cannot increase  $M_\beta$  ( $\beta < 1$ ), we have the inequality

$$\dot{M}_\beta \leq \beta M_{2\beta-1} + 1 - M_\beta(t). \quad (3.40)$$

Then, since  $\beta < 1$  implies  $2\beta - 1 < \beta$ , it is possible to show that for any value of a possible polydispersity exponent, we have in the scaling regime  $(M_\beta - \beta M_{2\beta-1}) \sim c M_\beta$ , where  $c$

is a strictly positive constant. In fact,  $M_\beta \gg M_{2\beta-1}$  and  $c = 1$  if  $\tau \leq 1 + \beta$ , while  $M_\beta \propto M_{2\beta-1}$  and  $c = 1/(\tau - 1 - \beta) - \beta/(\tau - 2\beta)$  if  $\tau > 1 + \beta$ . This result, combined with Eq. (3.40), leads to

$$\dot{M}_\beta \leq 1 - cM_\beta(t), \quad c > 0, \quad (3.41)$$

which shows that  $M_\beta$  cannot diverge. It is also clear that there is no way that  $M_\beta$  could become negative, since the smaller  $M_\beta$  is, the larger  $I(t)$  is. Therefore, if we rule out any pathological oscillatory behavior,  $M_\beta$  tends to a constant  $\bar{\phi}$ , which may possibly be zero. Now, if  $\bar{\phi} \neq 1$ , then the injection is asymptotically constant and, from Sec. III C, there is a critical steady state, with  $N(s) \sim 1/(s^{1+\beta} \ln s)$  at large  $s$ , and  $M_\beta$  diverges, which is contradictory (in addition, if  $\bar{\phi} > 1$ , the distribution is negative near  $s = 1$ ). Thus  $\bar{\phi} = 1$ , a nontrivial result that was a necessary condition for the mean field to correctly describe droplets models.

Now let us discuss the scaling properties of the equation. Since the injection term is vanishing, we expect the scaling equation (which describes large clusters) to be the same as in the case without injection. However, because of the fact that the cutoff  $s_0$  is constant and therefore negligible compared to  $S(t)$  we must select a solution different from the one obtained without injection.

To be more precise, we know that  $Y \sim S^2/t$  and that  $M_\beta$  has a finite limit. If we assume that there is polydispersity with  $\tau \geq 1 + \beta$ , these two conditions lead to  $S(t) \gg t^{1/(1-\beta)}$  and we find that the scaling equation is once again Eq. (3.25), which yields  $\tau \leq 1 + \lambda < 1 + \beta$ , in contradiction with our assumption. Thus  $\tau < 1 + \beta$  and  $M_\beta \propto tS(t)^{\beta-1}$ , leading to

$$\theta = 1 + \beta, \quad z = \frac{1}{1 - \beta}, \quad (3.42)$$

which correspond to the results previously obtained for droplets deposition and coalescence (with  $\beta = d/D$ ). The scaling equation is Eq. (A22), with positive  $a$  and  $b$ . This equation is nonlinear and is likely to admit several classes of solutions. We have seen that when there is no injection, a solution is selected that vanishes below a finite  $x_0 > 0$ . However, in the presence of injection the scaling function has no lower cutoff ( $x_0 = 0$ ) and we can have a polydispersity exponent.

To investigate the small- $x$  behavior of  $f$ , we introduce the auxiliary function  $\varphi(x) = x^{\beta-1}f(x)$ , which leads to a scaling equation

$$\begin{aligned} & 2x^{1-\beta}\varphi(x) + x^{2-\beta}\varphi'(x) - x\varphi'(x) - \varphi(x) \\ &= \varphi(x) \int_\varepsilon^{+\infty} \varphi(x_1)\bar{K}(x, x_1)dx_1 \\ & \quad - \frac{1}{2} \int_\varepsilon^{x-\varepsilon} \varphi(x_1)\varphi(x-x_1)\bar{K}(x_1, x-x_1)dx_1, \end{aligned} \quad (3.43)$$

where  $\bar{K}(x, y) = x^{1-\beta}y^{1-\beta}K(x, y)$  ( $\varepsilon$  is included to regularize the collision terms that are separately diverging in the  $\varepsilon \rightarrow 0$  limit [18]). We remark that the most diverging term for  $x \rightarrow 0$  on the left-hand side is  $-x\varphi'(x) - \varphi(x)$ , so that, as far as the determination of the asymptotic behavior  $\varphi(x) \propto x^{-\tau'}$

is concerned, we can straightforwardly generalize the results of van Dongen and Ernst [18,19]. The kernel  $\bar{K}$  has  $\bar{\lambda} = 2 + \lambda - 2\beta$  and  $\bar{\mu} = 1 + \mu - \beta$ , and we find that the function vanishes at small  $x$  for  $\bar{\mu} < 0$ ,  $\tau' = 1 + \bar{\lambda}$  for  $\bar{\mu} > 0$ , and  $\tau'$  is nontrivial, with

$$\tau' = 1 + \int_0^{+\infty} \varphi(x)x^{\bar{\lambda}}dx < 1 + \bar{\lambda} \quad (3.44)$$

for  $\bar{\mu} = 0$ . Therefore, for  $\mu < \beta - 1$ , we have no polydispersity, while for  $\mu > \beta - 1$  we have  $\tau = 2 + \lambda - \beta$  and for  $\mu = \beta - 1$

$$\tau = \beta + \int_0^{+\infty} f(x)x^{\lambda+1-\beta}dx < 2 + \lambda - \beta. \quad (3.45)$$

Now, for  $\lambda = 2\beta - 1$ , we find that  $\tau = 1 + \beta$  if  $\mu > \beta - 1$ , while  $\tau$  is nontrivial and strictly less than  $1 + \beta$  for  $\mu = \beta - 1$ . Hence, for  $\mu \leq \beta - 1$  the scaling theory is consistent, while for  $\mu > \beta - 1$  there is a contradiction with  $\tau < 1 + \beta$ . The latter case precisely corresponds to droplets deposition [see Eq. (2.13)]. However, a consistent scaling with a nontrivial polydispersity exponent could be obtained if we include pair correlations in the collision kernel and if the resulting kernel has  $\mu = \beta - 1$ .

This scenario is to be related to an early numerical work of Tanaka [43]. Tanaka solved a set of coupled differential equations describing growth and coalescence with renucleation for  $d = 2, D = 3$ . Dynamical pair correlations due to an excluded volume were included in an approximate form and Tanaka found a bimodal droplet mass distribution with a nontrivial polydispersity exponent, in agreement with the results described in Sec. II. It seems quite clear that his set of equations becomes equivalent to a Smoluchowski equation very similar to ours in the long-time limit, but with a collision kernel modified by correlations. It would be interesting to try to determine the kernel from his equation, although this seems to be quite a difficult task.

#### IV. HETEROGENEOUS GROWTH WITH POLYDISPERSITY

In Sec. III we found from a mean-field approach that the kinetics of heterogeneous growth with  $d = D$  (for instance, disks on a plane or spheres in three dimensions) should be qualitatively different from its counterpart with  $d < D$ . From the scaling theory of the generalized Smoluchowski equation, we found that there should be a transition from a monodisperse scaling function for  $\omega < 0$  to a polydisperse function with a nontrivial polydispersity exponent  $\tau$  for  $\omega \geq 0$ . This mean-field result is actually very interesting since it corroborates numerical simulations performed by Family and Meakin [9,5], who found that polydispersity occurs for  $d = D = 2$  and  $\omega = 0.5$ .

Thus our Smoluchowski equation approach sheds light on heterogeneous growth with  $d = D$ , which was not studied much due to the fact that interest was primarily focused on  $d = 2, D = 3$  relevant to breath figures and also to the fact that numerical simulations are much more difficult in this case (see below). In this section, first we discuss in detail what

should be expected from the mean-field theory and compute the polydispersity exponents for  $\omega \geq 0$ . Then we present some numerical simulations in  $d=2$  and discuss the relevance of the mean-field theory.

### A. Mean-field theory

In Sec. II B it was found that the collision kernel corresponding to heterogeneous growth with  $d=D$  was

$$K(x,y) = (x^{\omega/D} + y^{\omega/D})(x^{1/D} + y^{1/D})^{D-1}, \quad (4.1)$$

with  $\lambda = 1 + (\omega - 1)/D = \beta$ . The corresponding generalized Smoluchowski equation was found to be nongelling for  $\omega \leq 1$  and in the following we shall take  $\omega < 1$ .

The reason why growth with  $d=D$  is different in the mean field from  $d < D$  is rather subtle. As discussed in Sec. III, the competing dynamical mass scales corresponding to exogenous growth and growth by collision,  $S_g(t)$  and  $S_c(t)$ , respectively, are of the same order at long times for  $d=D$ , which leads to a marginal enhancement of the growth of the typical mass  $S(t)$  and to logarithmic mass growth

$$S(t) \propto (t \ln t)^{D/(1-\omega)}, \quad M_1(t) \sim \ln t. \quad (4.2)$$

This implies that the cutoff  $x_0 = \lim_{s \rightarrow 0} s(t)/S(t)$  in the scaling function is zero, in contrast to the  $d < D$  case for which  $x_0 > 0$ , and the scaling equation is the same as for Smoluchowski's equation without growth.

For  $\omega \geq 0$  we have  $\mu = 0$  and consequently there is a non-trivial polydispersity exponent  $\tau$ . We can use the methods discussed in [20] to study  $\tau$ . These methods make it possible to derive exact bounds and excellent approximations for  $\tau$ . The key relations that we use are, on the one hand, integral equation (3.27) for  $\tau$  and, on the other hand, a series of integral equations for the moments  $M_\alpha$  of  $\tau$  [18] obtained by multiplying Eq. (3.25) by  $x^\alpha$  and integrating over  $x$ , for any value of  $\alpha > \tau - 1$  (such that the integrals converge in zero):

$$2(1-\alpha) \int_0^\infty x^\alpha f(x) dx = \int \int_0^\infty f(x)f(y)K(x,y) \times [x^\alpha + y^\alpha - (x+y)^\alpha] dx dy. \quad (4.3)$$

As a preliminary remark, let us show that when  $D \geq 2$ , the exponent  $\tau$  is bigger than one. Let us assume that  $\tau < 1$ . Since the scaling function is integrable in zero, we can write Eq. (4.3) with  $\alpha = 0$ ,

$$2 \int_0^{+\infty} f(x) dx = \int \int_0^{+\infty} f(x)f(y)K(x,y) dx dy. \quad (4.4)$$

From the inequality,

$$K(x,y) = (x^{\omega/D} + y^{\omega/D})(x^{1/D} + y^{1/D})^{D-1} \geq x^\lambda + y^\lambda \quad (4.5)$$

for  $D \geq 2$ , we see that Eq. (4.4) leads to

$$\int_0^{+\infty} f(x) dx \geq \int_0^{+\infty} f(x) dx \int_0^{+\infty} y^\lambda f(y) dy, \quad (4.6)$$

TABLE II. Exact upper and lower bounds.

$\omega$	$\tau_m$	$\tau_M$
0.02	1.020	1.510
0.2	1.339	1.588
0.3	1.472	1.594
0.4	1.514	1.601
0.5	1.540	1.608
0.6	1.572	1.614
0.8	1.623	1.800
0.9	1.633	1.900

which, combined with Eq. (3.27), implies  $\tau \geq 1$ , in contradiction with our assumption.

One can also find better exact bounds. Combining Eqs. (3.27) and (4.3), one obtains

$$\tau = 2 - (1-\alpha) \frac{\int \int_0^\infty g(x,y) dx dy}{\int \int_0^\infty g(x,y) A(x/y) dx dy}, \quad (4.7)$$

with  $g(x,y) = f(x)f(y)(x^\alpha y^\lambda + x^\lambda y^\alpha)$  and  $A(u) = [1 + u^\alpha - (1+u)^\alpha]K(1,u)/(u^\alpha + u^\lambda)$ .

The ratio in Eq. (4.7) is the inverse of the average of  $A(x/y)$  with weight  $g(x,y)$ , so that computing the maximum  $M_\alpha$  and the minimum  $m_\alpha$  of  $A$  for various values of  $\alpha$  leads to exact bounds for  $\tau$  that can be used to check numerical evaluations of  $\tau$  [20] since Eq. (4.7) implies

$$2 - (1-\alpha)/m_\alpha \leq \tau \leq 2 - (1-\alpha)/M_\alpha. \quad (4.8)$$

As a concrete example, let us determine such bounds for  $D=2$  and  $\omega=0.5$ . Since  $\tau < 1 + \lambda$  (here  $\lambda=0.75$ ), Eq. (4.7) holds for  $\alpha = \lambda$ , for which we can numerically compute the minimum and maximum of  $A$ . From Eq. (4.8), this leads to the inequality  $1.5 \leq \tau \leq 1.607175$ . Thus Eq. (4.8) holds for  $0.607175 < \alpha \leq \lambda$  and we can compute new bounds for each  $\alpha$  in this interval and find the tightest bounds. The upper bound obtained for  $\alpha = \lambda$  cannot be improved since  $A(0) = 1$  for  $\alpha < \lambda$ , hence  $2 - (1-\alpha)/M_\alpha \geq 1 + \alpha$ , but we obtain a better lower bound of 1.54 for  $\alpha = 0.68$ . Table II presents such exact bounds for  $D=2$ .

The next step is to use a variational method to compute accurate values of  $\tau$  at very low numerical cost [20]. The basic idea of the variational approximation is to choose a parametrized family of variational functions and minimize the violation of Eq. (4.7) for a well-chosen sample of values of  $\alpha$ . The key point is the choice of the variational function. As argued in [20], a natural three parameters class of functions is

$$f_v(x, \tau_0, c_1, c_2) = \left( \frac{1}{x^{\tau_0}} + \frac{c_1}{x^{\tau_1(\tau_0)}} + \frac{c_2}{x^\lambda} \right) e^{-x}. \quad (4.9)$$

The last term corresponds to the exact asymptotic decay at large  $x$  of the scaling function [18,19], while  $\tau_0$  is the polydispersity exponent and  $\tau_1$  is the subleading exponent in small  $x$  (its value as a function of  $\tau_0$  is taken to be the same as for the exact scaling function). This class of function has the correct large- $x$  and small- $x$  asymptotic behavior expected

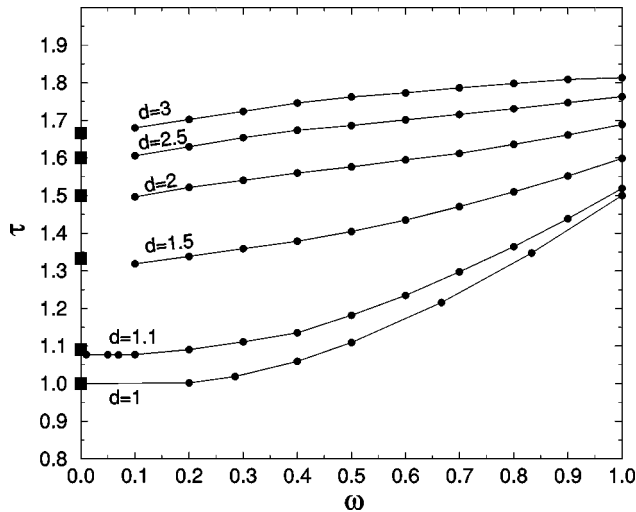


FIG. 4. Exponent  $\tau$  for the kernel  $(x^{\omega/D} + y^{\omega/D})^{D-1}$  computed with the variational approximation for  $\omega > 0$  and  $1 \leq D \leq 3$ . The theoretical  $\omega \rightarrow 0$  limit of  $\tau$ ,  $\tau_0 = 2 - 1/D$  is plotted on the Y axis (squares).

for the scaling function. In addition, it contains the exact scaling functions for  $K = 1$  and  $K = x + y$ , therefore the variational approximation yields the exact result for  $\tau$  in these cases (as checked in [20]).

A natural error function, measuring the violation of Eq. (4.7) for a set of  $n$  moments  $\alpha_i$ , is simply

$$\chi^2(f_v) = \sum_i [\tau_0 - G_{\alpha_i}(f_v)]^2, \tag{4.10}$$

where  $G_{\alpha_i}(f_v)$  is the right-hand side Eq. (4.7) for  $\alpha = \alpha_i$  and  $f = f_v$ . This error function is, by construction, strictly zero for the exact scaling function. For the chosen class of variational functions,  $G_{\alpha_i}(f_v)$  can be expressed in terms of  $\Gamma$  functions and simple one-dimensional integrals, which makes its numerical computation extremely fast [20].

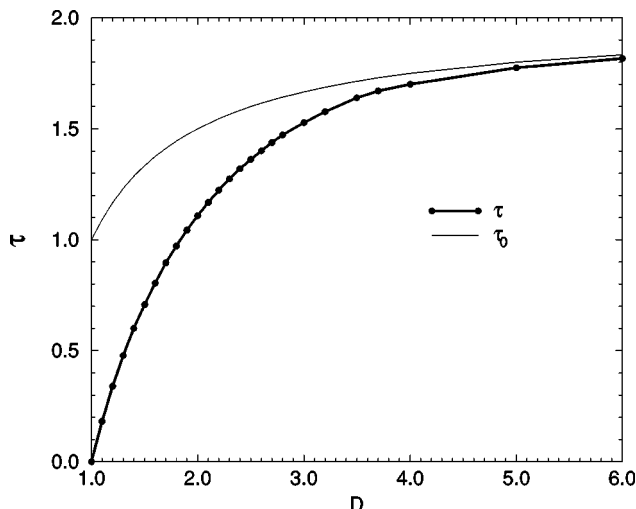


FIG. 5. Variational approximation for  $\tau$  when  $\omega = 0$ , compared to its  $\omega \rightarrow 0^+$  limit  $\tau_0 = 2 - 1/D$ . Both  $\tau$  and  $\tau_0$  tend to 2 when  $D \rightarrow \infty$ .

The variational approximation was used to study the behavior of  $\tau$ . The set of moments was chosen as discussed in [20]. Results are shown in Fig. 4 for different values of  $D$  and  $\omega > 0$ , while Fig. 5 shows the values of  $\tau$  for  $\omega = 0$ . For  $D = 1$ , the kernel is equal to  $x^\omega + y^\omega$ , corresponding to the kernel  $K_{1/\omega}^1$  with the notations of Eq. (3.28), which was extensively studied in [20]. The exponent  $\tau$  is bigger than 1 for any  $\omega > 0$ , while  $\tau = 0$  when  $\omega = 0$ . Since  $1 \leq \tau < 1 + \omega$  for  $\omega > 0$ , we see that  $\tau \rightarrow 1$  when  $\omega \rightarrow 0$ , hence  $\tau$  has a discontinuity at  $\omega = 0$ . For any  $D$  and  $\omega = 0$ , the kernel also reduces to  $K_D^{D-1}$ .

It appears that  $\tau$  has a discontinuity at  $\omega = 0$  not only for  $D = 1$ , but for  $D > 1$  as well: When  $\omega \rightarrow 0^+$ ,  $\tau$  has the limit  $\tau_0$  bigger than its value at  $\omega = 0$ . Thus the discontinuity that was rigorously shown to exist for  $D = 1$  pertains to  $D \geq 1$ . It is difficult to extract the value of  $\tau_0$  accurately since the variational algorithm appears to be less accurate for small values of  $\omega$  (for  $\omega$  typically less than 0.1). However,  $\tau_0$  seems to be close to  $2 - 1/D$ , which is the value of  $1 + \lambda$  at  $\omega = 0$ . Actually, a heuristic argument, inspired from the discussion for the  $K_D^d$  kernel in the large- $D$  ( $d > 1$ ) limit, yields  $\tau_0 = 2 - 1/D$ .

Let  $f_0(x)$  be the exact scaling function for  $\omega = 0$ . From Eq. (3.27) we get

$$\tau_0 = \tau_{\omega=0} + \lim_{\omega \rightarrow 0^+} \int_0^{+\infty} [f(x) - f_0(x)] x^{1+(\omega-1)/D} dx \tag{4.11}$$

and the limit on the right-hand side of Eq. (4.11) must be strictly positive, although  $[f(x) - f_0(x)] \rightarrow 0$  for any  $x > 0$ . How can this occur? Since  $\tau > \tau_{\omega=0}$  (for small  $\omega$ ),  $[f(x) - f_0(x)] \sim c/x^\tau$  when  $x \rightarrow 0$  and  $c$  must vanish when  $\omega \rightarrow 0$ . Thus the integral has an integrable singularity  $cx^{1+(\omega-1)/D-\tau}$ . If  $\tau_0 < 2 - 1/D$  (we know that  $\tau_0 \leq 2 - 1/D$  from  $\tau < 1 + \lambda$ ), the contribution of the singularity is wiped out by the vanishing of  $c$ , whereas, if  $\tau_0 = 2 - 1/D$ , the integral is equivalent to  $c/(\tau_0 + \omega/D - \tau)$  and it has the finite limit  $\tau_0 - \tau_{\omega=0}$  provided  $c$  vanishes as  $(\tau_0 - \tau_{\omega=0})(\tau_0 + \omega/D - \tau)$ .

Figure 5 plots the value of  $\tau$  and  $\tau_0 = 2 - 1/D$  for  $\omega = 0$  and  $1 \leq D \leq 6$ . Both  $\tau$  and  $\tau_0$  have the limit 2 when  $D \rightarrow \infty$ , which implies that the discontinuity in  $\omega = 0$  vanishes at large  $D$ , as can be seen on the figure. The reason why  $\tau \rightarrow 2$  is that when  $D \rightarrow \infty$ ,

$$K(x, y) = 2^D [(xy)^{1/2} + O(1/D)] \tag{4.12}$$

and therefore the  $D \rightarrow \infty$  limit of  $\tilde{f} = 2^D f$  is solution of Eq. (3.25) with the kernel  $(xy)^{1/2}$ , which is a  $\mu > 0$  kernel with exponent  $\tau = 2$  (the same trick was used in [20] to study the  $d \rightarrow \infty$ ,  $d = \lambda D$  limit for the  $K_D^d$  kernel).

For  $\omega < 0$ , we have  $\mu = \omega/D < 0$ , and using the results of van Dongen and Ernst [19], we have, for  $x \rightarrow 0$ ,

$$f(x) \sim B(\omega) x^{-\gamma(\omega)} \exp\left(\frac{D}{b(\omega)\omega} x^{\omega/D} \int_0^{+\infty} x^{1-1/D} f(x) dx\right), \tag{4.13}$$

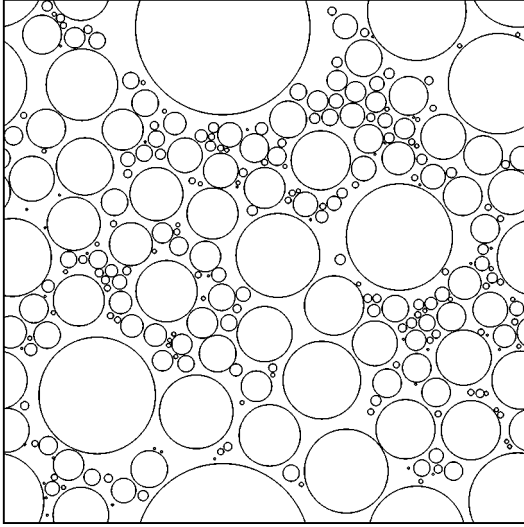


FIG. 6. Typical droplet configuration in the scaling regime of growth and coalescence with  $d=D=2$ , obtained here for  $\omega = -1$ , from 262 144 droplets of radius 0.75 in the initial condition on a  $1024 \times 1024$  lattice. The picture represents the whole system (with periodic boundary conditions) at  $t=5.0$  ( $S=7693.9$ ). The number of droplets has dropped to 287.

where  $B$ ,  $\gamma$ , and  $b = \lim_{\mu \rightarrow 0} S S^{-2-\lambda} Y$  are  $\omega$ -dependent constants. These constants also depend on the definitions of  $Y(t)$  and  $S(t)$ , but  $\gamma \rightarrow 2$  when  $\mu \rightarrow 0$ . For a given definition, say

$$S(t) = \langle s^2 \rangle / \langle s \rangle, \quad Y(t) = S^2 / M_1, \quad (4.14)$$

van Dongen and Ernst showed that the scaling function crosses over to the  $\mu=0$  (polydisperse) case when  $\mu \rightarrow 0$  since the small- $x$  asymptote tends to  $B(0)x^{-\tau}$ , where  $\tau = b^{-1} [2 - \int_0^{+\infty} x^{1-1/D} f(x) dx]$  is precisely the  $\mu=0$  polydispersity exponent [we had set  $b=1$  in Eq. (3.27)].

Consequently, we should observe this crossover in numerical simulation. Moreover, for small, but finite  $\omega$ , the critical  $x_c$  below which  $f(x)$  significantly departs from the power law corresponds to  $\mu \ln x_c$  of order one. Thus it is reasonable to expect a scaling behavior when  $\omega \rightarrow 0^-$ ,

$$f(x, \omega) = x_c(\omega)^{-\tau} g[x/x_c(\omega)], \quad (4.15)$$

with  $x_c(\omega) = \exp[-c/\omega + o(1/\omega)]$ ,  $g(y) \rightarrow 0$  at small  $y$ , and  $g(y) \propto y^{-\tau}$  at large  $y$ .

### B. Numerical simulations

The mean-field theory is in full agreement with the observation by Family and Meakin [9] and Meakin [5] of a polydispersity exponent in simulations with  $d=D=2$  and  $\omega = 1/2$ . To check the mean-field prediction of a transition from monodispersity to polydispersity at  $\omega=0$ , we have performed simulations in  $d=2$  for various values of the growth exponent  $\omega$ . In one step of the simulation, all the droplets radii were increased of an amount  $\delta r = r^\omega \delta t$  and then collisions were looked for and resolved. In most of the simulations, the time increase  $\delta t$  was equal to 0.005. It was chosen small enough such that further reduction would not lead to significant modification of the results. As can be intuitively understood, the number of droplets decreases much faster for

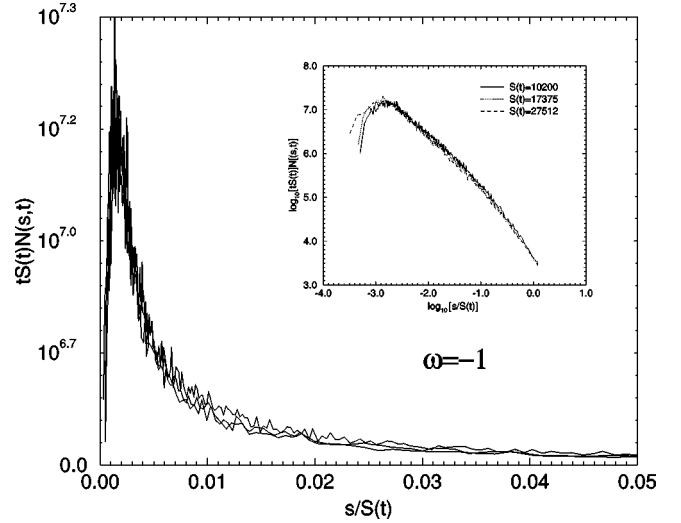


FIG. 7. Scaled mass distributions at three stages in the simulation of heterogeneous growth with  $\omega = -1$ . These results were obtained from 96 simulations. In each simulation, 262 144 droplets of radius 0.75 were initially randomly placed on a  $1024 \times 1024$  lattice (without overlap).

$d=D$  than for  $D>d$ . In the scaling regime, it was cut by a factor of more than 1000 and we were obliged to start from a huge number of droplets (about  $2.5 \times 10^5$ ) and perform a large number of simulations to obtain acceptable statistics, without being able to reach very large times. Figure 6 shows a configuration obtained at  $t=5.0$  for  $\omega = -1$  from an initial configuration of  $1024^2$  droplets. The scaling form Eq. (3.15) was used with  $Y = tS^{1+\beta}$  to obtain convincing data collapse for the mass distribution, as shown in Fig. 7. Although the distribution of masses looks quite broad in Fig. 6, the scaling function vanishes when  $x \rightarrow 0$ , in agreement with the mean-field theory.

Figure 8 plots the scaling functions for several values of  $\omega$ . The results are consistent with a transition from a small- $x$

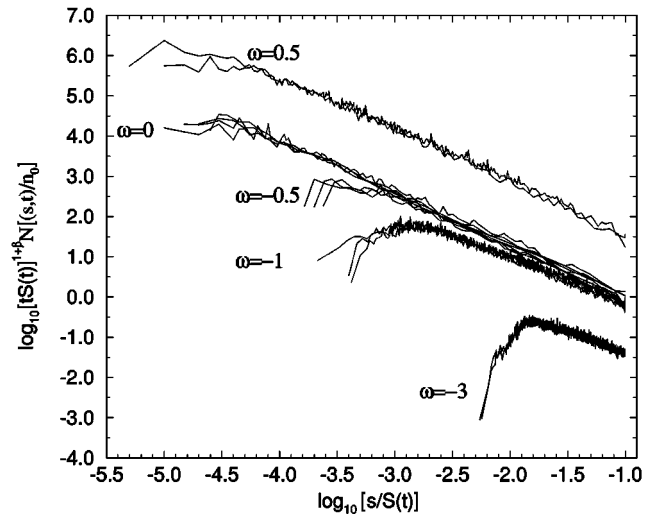


FIG. 8. Small  $x=s/S$  behavior of the scaled mass distributions obtained in numerical simulations for different values of the growth exponent  $\omega$ .  $N(s,t)$  was normalized by the total initial number of droplets  $n_0$ .

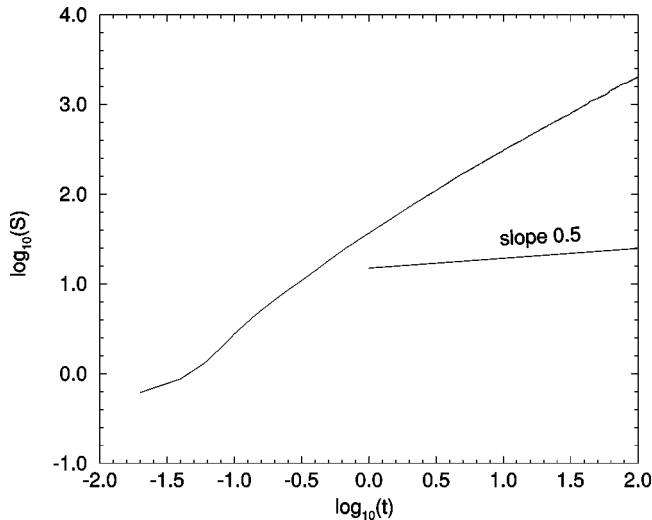


FIG. 9. For  $\omega = -3$ ,  $S(t)$  grows much faster than  $t^{D/(1-\omega)}$  (slope 0.5) even in the corresponding scaling regime ( $t > 50$ ), a behavior that may be related to logarithmic enhancement of  $S$  in the mean field.

diverging scaling function for  $\omega \geq 0$  to a small- $x$  vanishing scaling function for negative value of  $\omega$ . For the values of negative  $\omega$  considered, the scaling function, as visible in Fig. 7, although vanishing when  $x \rightarrow 0$ , is quite broad, with a maximum at a value  $x$  significantly smaller than 1. When  $\omega \rightarrow 0^-$ , we observe a crossover to the  $\omega = 0$  power law and the position of the maximum of the scaling function rapidly tends to zero when  $\omega \rightarrow 0$ , consistently with the discussion around Eq. (4.15). Moreover, the exponent extracted from the numerics is about 1.2, which compares well with  $\tau = 1.108$  from the mean field. However, the  $\tau$  exponents for  $\omega = 0$  and  $\omega = 0.5$  do not seem to be significantly different, in contrast with the quite large discontinuity in the mean field. Figure 9 shows the evolution of  $S(t)$  for  $\omega = -3$ . In the scaling regime,  $S(t)$  is seen to grow much faster than  $t^{D/(1-\omega)} = \sqrt{t}$ , which is consistent with the mean-field logarithmic enhancement.

Hence the mean-field approximation yields a qualitatively correct description of numerical results for  $d = D$ . However, this approximation is clearly bound to break down at very long times, probably unreachable so far to numerical simulations. The reason is that the mean field  $M_1(t)$  diverges, while the actual  $M_1(t)$  cannot diverge from a geometric constraint, which, of course, is absent in the mean-field theory. Indeed, for  $d = D$ ,  $M_1(t)$  is also proportional to the occupied area fraction and is therefore bounded. This means that at long times, strong density-density correlations and/or multiple collisions play a crucial role and are not taken into account in the mean-field theory. Consequently, the upper critical dimension is infinite for  $d = D$ . However, since the divergence of  $M_1$  is only marginal, the mean-field description should be essentially correct for  $t < t_c$ , where  $t_c$  is a large crossover time. Thus the qualitative agreement between the mean field and numerics can be explained by the fact that  $t_c$  is too large to be observed.

The mean-field approximation also breaks down for all  $d > D$  because the occupied surface fraction  $M_{d/D}$  algebraically diverges. Since the divergence is algebraic, we expect

the crossover time  $t_c$  to be much shorter than for  $d = D$ . In fact, the system is obviously gelling for  $d > D$  and all  $\omega$  since the occupied surface increases in a coalescence (which leads to avalanches of collisions). For instance, numerical simulations performed for  $d = 2$ ,  $\omega = -1$ , and  $D = 1.7$  show gelation at a finite time  $t_g \approx 0.12$ . The gelation time is nearly unaffected when doubling the mass of the sample, keeping the same initial density and mass of the droplets, or reducing the time step by a factor 2, and thus seems to be well defined in the continuous time and thermodynamic limit. This case corresponds to a nongelling system according to the mean-field gelling criterion  $d > D + 1 - \omega$ , which appears to be only a sufficient condition.

## V. CONCLUSION

In this article we have extensively studied a generalized Smoluchowski equation corresponding to aggregation processes for which particles (or clusters) grow between collisions, with  $\dot{s} = As^\beta$ , and small particles (monomers) are injected. A physical motivation for this work is droplet nucleation and we have derived generalized Smoluchowski equation directly and found the collision kernel for two models describing, respectively, homogeneous and heterogeneous nucleation.

For a generic kernel, with parameters  $\lambda, \mu$ , we have shown that the gelation criterion was  $\max(\lambda, \beta) > 1$ . We have devoted much time to the study of the equation *without injection*, for which we have provided two exact solutions. The scaling properties for a generic kernel are seen to be strongly affected by the exogenous growth term and depend on  $\beta$ ,  $\lambda$ , and  $\mu$ . For  $\lambda > \beta$ , however, the scaling is the same as for the standard equation. For the interesting case  $\lambda = \beta$ , the behavior of the typical mass  $S(t)$  is modified, but the scaling function is unchanged. For  $\lambda < \beta$ , the scaling function is qualitatively different and vanishes at a finite  $x_0 > 0$ .

We have also studied the case of a *constant injection rate* of monomers. The distribution reaches an asymptotic steady state with a power law tail  $N_\infty(s) \propto s^{-\tau}$  and we find that  $\tau$  depends on  $\beta$  and  $\lambda$ .

We have paid special attention to the case of a *constant mass injection rate* and  $\lambda = 2\beta - 1$ , related to homogeneous nucleation. This corresponds to a time-dependent, self-consistent injection rate  $I(t) \propto c - M_\beta(t)$ . We have shown that  $I(t)$  vanishes at long times, in agreement with the droplet deposition and coalescence model. For droplets deposition,  $M_\beta$  is proportional to the surface coverage and the vanishing of the injection rate corresponds to the saturation of the coverage to 1. Thus our self-consistent Smoluchowski equation recovers a merely geometrical constraint, which is quite nontrivial.

As far as scaling is concerned, we have found consistent results for  $\mu \leq \beta - 1$ , with nontrivial polydispersity exponents for  $\mu = \beta - 1$ , recovering  $\theta = 1 + \beta$  and  $z = 1/(1 - \beta)$  as for the droplets deposition and coalescence model. However, for  $\mu > \beta - 1$  kernels, we could not find a consistent scaling and there might be no scaling solution with a constant mass injection rate. The mean-field kernel for droplets deposition and coalescence has  $\mu > \beta - 1$  and taking into account excluded-volume pair correlations may be essential to obtain a consistent description by a kinetic equation, including a



nontrivial polydispersity exponent if  $\mu$  is switched to  $\beta-1$ . It is quite difficult though to study these correlations either numerically or analytically.

Finally, we have applied these results to droplet growth and coalescence with  $d=D$ . We have shown that Smoluchowski's approach accounts for the qualitative difference in the scaling function with the  $d<D$  case. We have computed nontrivial polydispersity exponents occurring for  $\omega\geq 0$  and described the crossover from monodispersity to polydispersity occurring for  $\omega\rightarrow 0^-$ . We have compared these theoretical results with numerical simulations, with good agreement, despite mean-field limitations, which we have discussed.

As a conclusion we would like to point out that one of the main reasons why people have become increasingly interested in breath figures is that it is an example of a *geometrically constrained* growth process, where diffusion plays a minor role, in contrast with diffusion-limited cluster-cluster aggregation [14,15,28] or Brownian coalescence of droplets [44]. Therefore, one could doubt that neglecting density-density correlations may have no dramatic consequences. Indeed, for homogeneous nucleation, we have seen that pair correlations may be crucial to finding a correct scaling function and we also found an infinite upper critical dimension for heterogeneous  $d\geq D$  nucleation. However, we have shown that Smoluchowski's equation in an extended form could be successfully used to describe heterogeneous growth for  $d<D$ , that it was qualitatively correct for  $d=D$  in the regime accessible to simulations, and that it also gives very interesting insights into homogeneous growth, which was not *a priori* obvious.

#### ACKNOWLEDGMENT

We are very grateful to P. L. Krapivsky for helpful correspondence.

#### APPENDIX: SCALING THEORY WITHOUT INJECTION

In this appendix we shall give a detailed demonstration of the scaling results given in Sec. III B 2 for the generalized Smoluchowski equation without injection of monomers. We assume that starting from a narrow distribution of droplets, the late-time solution of Eq. (3.1) has the scaling form of Eq. (3.15). In our demonstration, we shall always use the fact that  $S(t)$  cannot be negligible compared to  $s_0(t)\sim t^{1/(1-\beta)}$ , the lower cutoff, from the discussion in Sec. III B 2. We shall also implicitly assume that  $Y(t)$ ,  $S(t)$ , and all the moments of  $N(s,t)$  are asymptotically regular convex or concave functions.

##### 1. Within the nongelling domain

To start with, let us study the case  $\lambda<1$  and  $\beta<1$ , i.e., nongelling systems that are not on the gelling boundary. Our discussion is based on the fact that either  $S(t)\gg s_0(t)$  or  $S(t)\propto s_0(t)$ . We shall study the implications of both possibilities.

##### (a) Case $S\gg s_0$

Let us assume that  $S(t)\gg s_0(t)$  or, equivalently, that  $S^{\beta-1}\ll \dot{S}/S$ . We see that the growth term (3.22) is much smaller than Eq. (3.21) in the scaling limit and the scaling equation is,

$$bx f'(x) + af(x) = f(x) \int_0^{+\infty} f(x_1) K(x, x_1) dx_1 - \frac{1}{2} \int_0^x f(x_1) f(x-x_1) K(x_1, x-x_1) dx_1 \quad (\text{A1})$$

where  $b = \lim \dot{S} S^{-2-\lambda} Y$  and  $a = \lim \dot{Y} S^{-1-\lambda}$  are positive and possibly zero or infinite.

For finite  $a$  and  $b$ , this equation is very close to the standard Smoluchowski equation (1.1) with the same kernel  $K$ , which corresponds to  $a=2b$  and  $0 < a < +\infty$  and was well studied in the literature [18–20]. The polydispersity exponent  $\tau$ , if any, has the upper bound  $\tau \leq 1 + \lambda < 2$  (see Sec. III B 3). As a consequence, from Eq. (3.18) we have

$$M_1(t) \propto S^2/Y. \quad (\text{A2})$$

From Eq. (3.24) we see that  $M_1(t)$  is nondecreasing. Thus  $M_1(t)$  either tends to a finite limit or goes to infinity.

(i) If  $M_1(t)$  tends to a finite limit, then, necessarily from Eq. (A2),  $Y \propto S^2$ . The scaling of Eq. (3.21) with Eq. (3.23) requires  $\dot{S} \propto S^\lambda$ , hence

$$S(t) \propto t^{1/(1-\lambda)}. \quad (\text{A3})$$

To be consistent with our assumption that  $S(t)\gg t^{1/(1-\beta)}$ , we must have  $\lambda > \beta$ . In addition, from Eq. (3.24), a necessary condition for  $M_1(t)$  to have a large- $t$  finite limit is that  $M_\beta(t)$  must be an integrable function. If  $\tau < 1 + \beta$ ,  $M_\beta$  scales as  $S^{1+\beta}/Y$ , i.e.,  $M_\beta \propto t^{(\beta-1)/(1-\lambda)}$ , and is integrable since  $\lambda > \beta$ .

If  $\tau > 1 + \beta$ , we have, from Eq. (3.19),

$$M_\beta \propto S(t)^{\tau-2} s_0(t)^{1+\beta-\tau} \ll s_0(t)^{\beta-1} \propto t^{-1} \quad (\text{A4})$$

since  $\tau < 2$  and  $S(t)\gg s_0(t)$ . Therefore,  $M_\beta$ , being equivalent to a power law much less than  $1/t$ , is integrable. If  $\tau = 1 + \beta$ , from Eq. (3.20),

$$M_\beta \propto S(t)^{\beta-1} \ln(S/s_0) \propto t^{(\beta-1)/(1-\lambda)} \ln t, \quad (\text{A5})$$

which is integrable when  $\lambda > \beta$ .

(ii) Now let us consider the case when  $M_1(t)$  diverges at long times. From Eqs. (3.24), (A2), (3.19), and (3.20) we obtain

$$\dot{M}_1 \propto \begin{cases} M_1 S^{\beta-1} & \text{if } \tau < 1 + \beta \\ M_1 S^{\tau-2} s_0(t)^{1+\beta-\tau} & \text{if } \tau > 1 + \beta \\ M_1 S^{\beta-1} \ln(S/s_0) & \text{if } \tau = 1 + \beta. \end{cases} \quad (\text{A6})$$

In the three cases,  $S\gg s_0$  implies that  $\dot{M}_1 \ll M_1 s_0^{\beta-1}$ , hence

$$\dot{M}_1 \ll \frac{M_1}{t}. \quad (\text{A7})$$

Therefore,  $M_1(t) \ll t^\alpha$  for any  $\alpha > 0$ . From Eq. (A2) and the fact that  $\dot{S}/S$  is at least of order  $1/t$  since  $S(t) \gg t^{1/(1-\beta)}$ , Eq. (A7) requires that

$$2\frac{\dot{S}}{S} \sim \frac{\dot{Y}}{Y}. \tag{A8}$$

Thus the scaling condition between Eqs. (3.21) and (3.23) is simply

$$\frac{\dot{S}}{S} \propto \frac{S^{1+\lambda}}{Y} \propto M_1 S^{\lambda-1}, \tag{A9}$$

which implies that  $S^{1-\lambda}$  is dominated by a power law. Combined with the fact that  $S(t) \gg t^{1/(1-\beta)}$ , this requires that

$$\frac{\dot{S}}{S} \propto \frac{1}{t} \tag{A10}$$

and

$$M_1 \propto t^{-1} S^{1-\lambda} \gg t^{(\beta-\lambda)/(1-\beta)}, \tag{A11}$$

thus, from Eq. (A7), we must have  $\lambda \geq \beta$ . Now, combining Eqs. (A11) and (A6), we see that

$$\dot{M}_1 \propto M_1^{-\alpha_1} t^{-\alpha_2} [\ln(t^{(\lambda-\beta)/(1-\beta)} M_1)]^{\alpha_3} \tag{A12}$$

( $\alpha_3 = 1$  if  $\tau = 1 + \beta$ ; otherwise  $\alpha_3 = 0$ ), where

$$\alpha_2 = \begin{cases} \frac{1-\beta}{1-\lambda} & \text{if } \lambda \leq \beta \\ \frac{2-\tau}{1-\lambda} + \frac{\tau-1-\beta}{1-\beta} & \text{if } \tau > 1 + \beta. \end{cases} \tag{A13}$$

Since  $M_1 \rightarrow \infty$ , the right-hand side of Eq. (A12) must be nonintegrable and as  $M_1$  is much smaller than any positive power of  $t$ , this implies that  $\alpha_2 \leq 1$ . Since  $\tau \leq 1 + \lambda$ ,  $\alpha_2 > 1$  if  $\lambda > \beta$ . Therefore, we must have  $\lambda \leq \beta$ . However, we already found that  $\lambda \geq \beta$ , thus  $\lambda$  must be equal to  $\beta$ . As a consequence,  $\tau$  is never bigger than  $1 + \beta = 1 + \lambda$  and we can distinguish between  $\mu > 0$  kernels, for which  $\tau = 1 + \lambda = 1 + \beta$ , and  $\mu \leq 0$  kernels, for which there is no polydispersity exponent or  $\tau < 1 + \beta$ .

Let us start with  $\mu \leq 0$  kernels. As  $\tau < 1 + \beta$  and  $\lambda = \beta$ , Eq. (A12) is reduced to  $\dot{M}_1 \propto 1/t$ , which leads to

$$M_1(t) \propto \ln t. \tag{A14}$$

For a  $\mu > 0$  kernel,  $\tau = 1 + \lambda = 1 + \beta$  and Eq. (A12) leads to

$$\dot{M}_1 \propto (\ln M_1)/t; \tag{A15}$$

it is easily seen that

$$M_1(t) \propto (\ln t) \ln(\ln t). \tag{A16}$$

In both cases, we have

$$S(t) \propto (t M_1)^{1/(1-\beta)}, \tag{A17}$$

$$Y(t) \propto S^2/M_1. \tag{A18}$$

Thus the initial assumption that  $S(t) \gg s_0(t)$  implies that  $\lambda \geq \beta$  and that the scaling equation is Eq. (A1) with  $a = 2b$  (since  $2\dot{S}/S \sim \dot{Y}/Y$ ) and  $0 < a < +\infty$  and is the same as for the standard Smoluchowski equation with the same kernel.

**(b) Case  $S \propto s_0$**

Conversely, let us assume that  $S(t) \propto t^{1/(1-\beta)}$ . If  $\dot{Y}/Y \gg \dot{S}/S \propto 1/t$ ,  $Y$  increases faster than any power law, the growth term is still negligible at long times, and Eqs. (3.21) and (3.23) are of the same order, hence  $S^{1+\lambda}/Y \propto \dot{Y}/Y$ , which is contradictory, for  $S^{1+\lambda}/Y$  vanishes faster than any power law while  $\dot{Y}/Y \gg 1/t$ .

Thus  $\dot{Y}/Y = O(\dot{S}/S)$  and both terms on the right-hand side of Smoluchowski's equation are of the same order at long times as  $\dot{S}/S \propto S^{\beta-1}$ . In addition, both terms must scale as the collision term; otherwise the obtained scaling equation has no physical solution vanishing below a finite argument  $x_0 > 0$ . Thus Eqs. (3.22) and (3.23) must be of the same order, which yields

$$\frac{S^{\beta-1}}{Y} \propto \frac{S^{1+\lambda}}{Y^2} \tag{A19}$$

and  $Y(t) \propto S(t)^{2+\lambda-\beta}$ . The fact that the scaling function vanishes at a finite  $x_0 > 0$  ensures that  $M_1(t) \propto S^2/Y$ , hence

$$M_1(t) \propto S(t)^{\beta-\lambda}. \tag{A20}$$

Since  $M_1(t)$  is nondecreasing, we must have  $\lambda \leq \beta$ . However, if  $\lambda = \beta$ , Eq. (3.3) yields

$$\dot{M}_1 \propto 1/t, \tag{A21}$$

hence  $M_1(t) \propto \ln t$ , which is in contradiction with Eq. (A20). Therefore, one must have  $\lambda < \beta$ . The scaling equation has the form

$$\begin{aligned} & b[\theta f(x) + x f'(x)] - a[x^\beta f(x)]' \\ &= f(x) \int_0^{+\infty} f(x_1) K(x, x_1) dx_1 \\ & \quad - \frac{1}{2} \int_0^x f(x_1) f(x-x_1) K(x_1, x-x_1) dx_1. \end{aligned} \tag{A22}$$

**(c) Conclusion**

Since  $S(t) \geq s_0(t)$ , the collection of the two cases we examined above leads to the conclusion that if  $\lambda < 1$  and  $\beta < 1$ , there are three main regimes of scaling, in agreement with the qualitative discussion in Sec. III B 2. If  $\beta > \lambda$ ,  $S(t)$  scales as  $S_g(t) \propto t^{1/(1-\beta)}$ ,  $Y(t) \propto S(t)^\theta$ , with  $\theta = 2 + \lambda - \beta$ , and there is no polydispersity exponent since the scaling function is zero below a finite  $x_0$ . If  $\beta < \lambda$ ,  $S(t)$  scales as  $S_c(t) \propto t^{1/(1-\lambda)}$ , the mass is asymptotically conserved, i.e.,  $M_1(t)$  tends to a constant, and  $\theta = 2$ . There can be a polydispersity exponent, which is the same as for the standard Smoluchowski equation (1.1) with the same kernel.

Eventually, in the marginal case when  $\lambda = \beta$ , the scaling of  $S(t)$  depends on the kernel not only through its homoge-

neity  $\lambda$ , but also through its  $\mu$  exponent. As in the  $\beta < \lambda$  case, the scaling equation is the same as for Smoluchowski's equation with the same kernel. For  $\mu \leq 0$  kernels, the mass in the system  $M_1(t) \propto \ln t$ , while for  $\mu > 0$  kernels, with  $\tau = 1 + \lambda$ ,  $M_1(t) \propto t(\ln t)\ln(\ln t)$ . In both cases,  $S \propto (tM_1)^{1/(1-\beta)}$  and  $Y \propto S^2/M_1$ .

These scaling results can be compared to the case  $K = 1$ ,  $\beta = 0$ , which we solved exactly. We found that the conventional scaling breaks down, that, with the proper scaling form, the scaling function is the same as for the exactly solvable standard Smoluchowski equation without the growth term, and that  $S(t) \propto (t \ln t)$ ,  $M_1(t) \propto \ln t$ , and  $Y \propto t^2 \ln t$ , just as predicted by the scaling theory.

## 2. $\lambda = 1$ and $\beta < 1$

For  $\lambda = 1$  and  $\beta < 1$ , it is possible to follow the same line of reasoning, with a few modifications. In this case, one has to distinguish between  $\mu > 0$  and  $\mu \geq 0$  (this is also true for the standard Smoluchowski equation with  $\lambda = 1$  [19]) since for  $\mu > 0$ , we find  $\tau = 2$  and the scaling of  $M_1$  has an extra  $\ln(S/s_0)$ . It is found that  $M_1$  is asymptotically conserved,  $S(t) \geq s_0(t)$ , and the scaling equation is Eq. (A1) with  $a = 2b < +\infty$ . For  $\mu > 0$ , one has  $\dot{S} \propto S/(\ln S)$ , which leads to

$$S(t) \propto e^{b\sqrt{t}}, \quad (\text{A23})$$

whereas if  $\mu \leq 0$ ,

$$S(t) \propto e^{bt}, \quad (\text{A24})$$

where  $b$  cannot be derived from the scaling theory.

## 3. $\beta = 1$ and $\lambda < 1$

In this case  $s_0(t) \propto e^t$  and the discussion is quite different. From Eq. (3.24) we see that

$$M_1(t) = M_1(0)e^t. \quad (\text{A25})$$

Since  $S(t) \geq s_0(t) \propto e^t$ , we have in the long-time limit  $\dot{S}/S \geq 1$ . Let us assume that  $\dot{S}/S \geq 1$ , i.e., that  $S(t)$  is bigger than any exponential function  $e^{at}$ , which means that Eq. (3.21) is much bigger than Eq. (3.22) (which scales as  $1/Y$  since  $\beta = 1$ ). From Eqs. (3.18), (3.19), and (3.20) it is clear that

$$S^2/Y = O(M_1(t)) = O(e^t). \quad (\text{A26})$$

Consequently, if Eq. (3.21) scales as Eq. (3.23), then  $\dot{S}/S^\lambda = O(e^t)$  and  $\dot{Y}/Y^{(1+\lambda)/2} = O(e^{t/2})$ . Since  $\lambda < 1$ , these two relations are in contradiction with the assumption that  $S$  is much bigger than any exponential function [which implies the same property for  $Y$ , through Eq. (A26)]. We see that if  $\dot{S}/S \geq 1$ , Eq. (3.21) is the leading term in the scaling limit and the scaling function is a pure power law  $f(x) = cx^{-\tau}$  with  $\tau = \lim(\dot{Y}/Y)(S/\dot{S})$ . One must have  $\tau > 2$  such that the total mass in the system is finite at finite times in the scaling regime. Making use of Eq. (3.19), we find that  $n(t) \propto M_1(t)/s_0(t)$  would tend to a finite value  $n_\infty > 0$ , which is unphysical.

Therefore,  $\dot{S}/S$  is of order 1. From arguments very similar to those we just used, it is easily seen that  $\dot{Y}/Y$  cannot be much bigger than 1. Thus, Eq. (3.21) scales as Eq. (3.22). If  $\dot{Y}/Y \rightarrow 1$  and  $\dot{S}/S \rightarrow 1$ , the left-hand side of Eq. (3.1) vanishes and we have to take into account the subleading terms in the scaling limit. This occurs for  $\lambda = 0$ , as will be seen below.

If the left-hand side does not vanish, the scaling with Eq. (3.23) leads to  $S^{1+\lambda} \propto Y$  and the scaling equation is once again Eq. (A1), but now with  $b/a = (1 - \dot{S}/S)/(1 - \dot{Y}/Y)$ . Consequently, the polydispersity exponent, if any, is less than  $1 + \lambda$  and Eq. (A2) holds, leading to  $S^2 \propto Y e^t$ . Since  $S^{1+\lambda} \propto Y$ , we have

$$S(t) \propto e^{t/(1-\lambda)}, \quad (\text{A27})$$

$$Y(t) \propto S^2 e^{-t}, \quad (\text{A28})$$

which excludes  $\lambda < 0$ , since  $S(t) \geq s_0(t) = e^t$ , and also  $\lambda = 0$  for which  $\dot{S}/S \rightarrow 1$  and  $\dot{Y}/Y \rightarrow 1$ . Note that in the  $\lambda > 0$  case, we find  $a = 2b$  and once again the scaling equation is the same as for the standard Smoluchowski equation.

Indeed, for the exactly solvable case  $K = 1$ ,  $\beta = 1$ , which corresponds to  $\lambda = 0$ , we found that  $S(t) \propto t e^t$  and  $Y(t) \propto S^2/e^t$ , thus  $\dot{S}/S \rightarrow 1$  and  $\dot{Y}/Y \rightarrow 1$ . Thus, to treat the  $\lambda = 0$  case, we shall write  $S(t) = X(t)M_1(t)$ , with  $\dot{X}/X \ll 1$ , and we have  $Y \propto S^2/M_1 = XS$ . The right-hand side of Eq. (3.1) scales as

$$-\frac{1}{Y}[2f(x) + xf'(x)]\frac{\dot{X}}{X}, \quad (\text{A29})$$

while the left-hand side scales as

$$\frac{S}{Y^2}(\dots) \propto \frac{X}{Y}(\dots), \quad (\text{A30})$$

which leads to  $X(t) \propto t$ , recovering the exact result for  $K = 1$ . Once again the scaling function is Eq. (A1) with  $a = 2b < +\infty$ . The polydispersity exponent  $\tau$  is strictly less than 2, which justifies *a posteriori* that  $Y \propto S^2/M_1$  (it is possible to show that assuming  $\tau > 2$  leads to a contradiction). However, for  $\lambda < 0$ , we were unable to find a consistent scaling.

## 4. $\lambda = 1$ and $\beta = 1$

In this case we still have  $M_1(t) \propto e^t$  and  $s_0(t) \sim e^t$ , but it is easily seen with the same kind of arguments as above that one must have  $\dot{S}/S \geq 1$ . Thus the exogenous growth term (3.22) is negligible and the scaling of Eqs. (3.21) and (3.22) yields  $\dot{S}/S \propto S^2/Y$ .

For  $\mu \leq 0$  kernels, one has  $M_1 \propto S^2/Y$  and we obtain  $\dot{S}/S \propto e^t$ , leading to

$$S(t) \propto e^{be^t}. \quad (\text{A31})$$

For  $\mu > 0$ , we have  $\tau = 2$  and  $M_1 \propto S^2 \ln(S/e^t)/Y$ , leading to  $\dot{S}/S \propto e^t/\ln(S)$  and

$$S(t) \propto e^{b\sqrt{e^t}}. \quad (\text{A32})$$

In these expressions  $b$  is an unknown positive constant.

- [1] S. K. Friedlander, *Smoke, Dust and Haze* (Wiley Interscience, New York, 1977).
- [2] *Kinetics of Aggregation and Gelation*, edited by F. Family and D. Landau (North-Holland, Amsterdam, 1984).
- [3] *On Growth and Form*, edited by H. E. Stanley and N. Ostrowsky (Nijhoff, Amsterdam, 1986).
- [4] T. Vicsek, *Fractal Growth Phenomena*, 2nd ed. (World Scientific, Singapore, 1992).
- [5] P. Meakin, Rep. Prog. Phys. **55**, 157 (1992).
- [6] D. Beysens and C. Knobler, Phys. Rev. Lett. **57**, 1433 (1986).
- [7] R. Vincent, Proc. R. Soc. London, Ser. A **321**, 53 (1971).
- [8] F. Family and P. Meakin, Phys. Rev. Lett. **61**, 428 (1988).
- [9] F. Family and P. Meakin, Phys. Rev. A **40**, 3836 (1989).
- [10] D. Fritter, C. Knobler, and D. Beysens, Phys. Rev. A **43**, 2858 (1991).
- [11] B. Derrida, C. Godrèche, and I. Yekutieli, Phys. Rev. A **44**, 6241 (1991).
- [12] B. Briscoe and K. Galvin, Phys. Rev. A **43**, 1906 (1991).
- [13] M. Marcos-Martin, D. Beysens, J.-P. Bouchaud, C. Godrèche, and I. Yekutieli, Physica A **214**, 396 (1995).
- [14] P. Meakin, Phys. Rev. Lett. **51**, 1119 (1983).
- [15] M. Kolb, R. Botet, and R. Jullien, Phys. Rev. Lett. **51**, 1123 (1983).
- [16] M. von Smoluchowski, Z. Phys. Chem. (Munich) **92**, 129 (1918).
- [17] P. G. J. van Dongen, Phys. Rev. Lett. **63**, 1281 (1989).
- [18] P. G. J. van Dongen and M. H. Ernst, Phys. Rev. Lett. **54**, 1396 (1985).
- [19] P. G. J. van Dongen and M. H. Ernst, J. Stat. Phys. **50**, 295 (1987).
- [20] S. Cueille and C. Sire, Phys. Rev. E **55**, 5465 (1997).
- [21] S. Cueille and C. Sire, Europhys. Lett. **40**, 239 (1997).
- [22] P. Krapivsky and S. Redner, Phys. Rev. E **54**, 3553 (1996).
- [23] R. M. Ziff, M. H. Ernst, and E. M. Hendriks, J. Colloid Interface Sci. **100**, 220 (1984).
- [24] M. H. Ernst, R. M. Ziff, and E. M. Hendriks, J. Colloid Interface Sci. **97**, 266 (1984).
- [25] F. Leyvraz and H. Tschudi, J. Phys. A **15**, 1951 (1982).
- [26] E. Hendriks, M. Ernst, and R. Ziff, J. Stat. Phys. **31**, 519 (1983).
- [27] D. S. Krivitsky, J. Phys. A **28**, 2025 (1995).
- [28] P. Meakin, Phys. Scr. **46**, 46 (1992).
- [29] J. Klett, J. Atmos. Sci. **32**, 380 (1975).
- [30] P. H. McMurry, J. Colloid Interface Sci. **78**, 513 (1980).
- [31] W. H. White, J. Colloid Interface Sci. **87**, 204 (1982).
- [32] J. G. Crump and J. H. Seinfeld, J. Colloid Interface Sci. **90**, 469 (1982).
- [33] E. M. Hendriks, J. Phys. A **17**, 2299 (1984).
- [34] E. M. Hendriks and R. M. Ziff, J. Colloid Interface Sci. **105**, 247 (1985).
- [35] T. Vicsek, P. Meakin, and F. Family, Phys. Rev. A **32**, 1122 (1985).
- [36] Z. Rácz, Phys. Rev. A **32**, 1129 (1985).
- [37] H. Hayakawa, J. Phys. A **20**, L801 (1987).
- [38] P. Bak, C. Tang, and K. Wiesenfeld, Phys. Rev. Lett. **59**, 381 (1987).
- [39] D. Dhar, Phys. Rev. Lett. **64**, 1613 (1990).
- [40] H. Takayasu, I. Nishikawa, and H. Tasaki, Phys. Rev. A **37**, 3110 (1988).
- [41] H. Takayasu, Phys. Rev. Lett. **63**, 2563 (1989).
- [42] S. N. Majumdar and C. Sire, Phys. Rev. Lett. **71**, 3729 (1993).
- [43] H. Tanaka, J. Heat Transfer **97**, 72 (1975).
- [44] P. Meakin, in *Dynamics and Patterns in Complex Fluids*, edited by A. Onuki and K. Kawasaki, Proceedings in Physics Vol. 52 (Springer, Berlin, 1990).